WL-TR-97-4081

ENVIRONMENTAL EFFECTS ON POLYMER-MATRIX COMPOSITES

C. W. Lee
B. P. Rice
K. E. G. Thorp

University of Dayton Research Institute
300 College Park Avenue
Dayton, Ohio 45469-0168

JUNE 1997

FINAL REPORT FOR PERIOD 14 SEPTEMBER 1995 – 28 APRIL 1997

Approved for public release; distribution unlimited

MATERIALS & MANUFACTURING DIRECTORATE
AIR FORCE RESEARCH LABORATORY
AIR FORCE MATERIEL COMMAND
WRIGHT-PATTERSON AIR FORCE BASE, OH 45433-7734

NOTICE

When government drawings, specifications, or other data are used for any purpose other than in connection with a definitely Government-related procurement, the United States Government incurs no responsibility or any obligation whatsoever. The fact that the government may have formulated or in any way supplied the said drawings, specifications, or other data, is not to be regarded by implication, or otherwise in any manner construed, as licensing the holder, or any other person or corporation; or as conveying any rights or permission to manufacture, use, or sell any patented invention that may be related thereto.

This report is releasable to the National Technical Information Service (NTIS). At NTIS, it will be available to the general public, including foreign nations.

This technical report has been reviewed and is approved for publication.

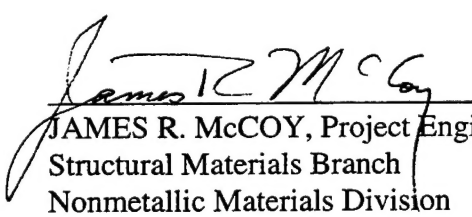

JAMES R. McCOY, Project Engineer
Structural Materials Branch
Nonmetallic Materials Division

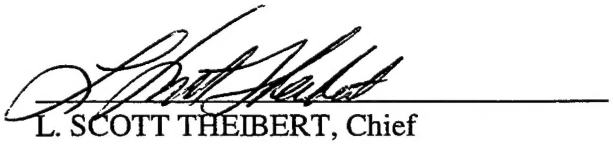

L. SCOTT THEIBERT, Chief
Structural Materials Branch
Nonmetallic Materials Division

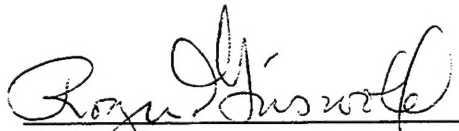

ROGER D. GRISWOLD, Assistant Chief
Nonmetallic Materials Division
Materials Directorate

Copies of this report should not be returned unless return is required by security considerations, contractual obligations, or notice on a specific document.

REPORT DOCUMENTATION PAGE

Form Approved
OMB No. 0704-0188

1. AGENCY USE ONLY *(Leave blank)*	2. REPORT DATE	3. REPORT TYPE AND DATES COVERED
	June 1997	Final Report - 14 Sep 95-28 Apr 97

4. TITLE AND SUBTITLE
ENVIRONMENTAL EFFECTS ON POLYMER-MATRIX COMPOSITES

5. FUNDING NUMBERS
F33615-95-D-5029
PE 61102F
PR 4347
TA 34
WU 10

6. AUTHOR(S)
C. W. Lee, B. P. Rice, and K. E. G. Thorp

7. PERFORMING ORGANIZATION NAME(S) AND ADDRESS(ES)
University of Dayton Research Institute
300 College Park Avenue
Dayton, OH 45469-0168

8. PERFORMING ORGANIZATION REPORT NUMBER
UDR-TR-97-94

9. SPONSORING/MONITORING AGENCY NAME(S) AND ADDRESS(ES)
Materials & Manufacturing Directorate
Air Force Research Laboratory
Air Force Materiel Command
Wright-Patterson Air Force Base, OH 45433-7734
POC: James R. McCoy, AFRL/MLBC, 937-255-9063

10. SPONSORING/MONITORING AGENCY REPORT NUMBER
WL-TR-97-4081

11. SUPPLEMENTARY NOTES

12a. DISTRIBUTION/AVAILABILITY STATEMENT
Approved for public release; distribution unlimited.

12b. DISTRIBUTION CODE

13. ABSTRACT *(Maximum 200 words)*

A variety of environmental factors can influence the performance of advanced polymers and composites. In particular, exposure to a combination of moisture and elevated temperature can significantly alter properties. The extent of chemical and physical changes is a function of exposure time and the temperature and humidity of the environment. This work discusses the effects of chemical and physical aging of AFR700B, a high-temperature addition polyimide resin. Neat resin samples were isothermally aged for 500 and 1000 hours at 250°C in dry air, humid air, and dry nitrogen. Changes in the dynamic mechanical properties and weight of the resin samples after these different exposures are discussed. An accelerated aging process was developed to facilitate the study of hydrolytic degradation. The effect of degradation on the T_g, weight, and mechanical behavior is discussed. The use of a silicon-nitride moisture barrier proved ineffective.

14. SUBJECT TERMS	15. NUMBER OF PAGES
environmental degradation, composites, hydrolysis, glass transition temperature, thermooxidative degradation, accelerated aging, isothermal aging, relaxation spectra, thermo-mechanical analysis, AFR700B, polyimide, neat resin	53
	16. PRICE CODE

17. SECURITY CLASSIFICATION OF REPORT	18. SECURITY CLASSIFICATION OF THIS PAGE	19. SECURITY CLASSIFICATION OF ABSTRACT	20. LIMITATION OF ABSTRACT
Unclassified	Unclassified	Unclassified	SAR

CONTENTS

FIGURES

FIGURES (Concluded)

EXECUTIVE SUMMARY

A variety of environmental factors can influence the performance of advanced polymers and composites. Exposure to moisture and high temperatures can lead to physical and chemical changes in the material which can, in turn, result in changes in the mechanical performance of the material. This work looked at a variety of issues involved in the hygrothermal degradation of norbornene-terminated addition polyimides. The material studied was AFR700B, a high glass transition temperature polyimide.

The effect of isothermal aging in a moist and dry environment was investigated through changes in the thermomechanical spectra, relaxation spectra, glass transition temperature, relative crosslink density, and specimen weights. The thermomechanical and relaxation spectra data suggested that physical aging occurred in all the aged specimens in a similar manner, regardless of the aging environment. Increases in the apparent rubbery modulus of the as-cured specimens provided evidence of additional crosslinking occurring during aging at 250°C. The magnitude of these changes was reduced in specimens aged in humid air, probably due to competing influences of moisture-induced chemical breakdown of the molecular structure. The decline in glass transition temperature of postcured specimens, and the appearance of additional features in the relaxation spectra of specimens aged in humid air, support the suggestion of molecular breakdown under prolonged hygrothermal exposure. Weight loss of the specimens suggested that the presence of moisture in the aging environment enhanced the thermooxidative degradation process.

Since hydrolytic degradation involves both moisture diffusion and chemical degradation, the two processes were studied independently. An accelerated aging process was developed to study the effect of hydrolytic degradation without consideration for diffusion. Using the

accelerated technique, it was shown that a polyimide can experience a decline in glass transition temperature after exposure to saturated steam at a temperature as low as 100°C. In addition, exposure of specimens to temperatures above 200°C in saturated steam resulted in severe degradation. Specimen mechanical properties declined as a result of hygrothermal exposure. The ultimate strength at 250°C was reduced by 38 percent after aging in saturated steam at 150°C for 48 hours. In addition, the ultimate strength at 300°C was reduced by 49 percent after aging in saturated steam at 150°C for 48 hours.

Moisture diffusivity was modeled using absorption and desorption, and attempts to limit diffusion through the use of a silicon nitride coating proved ineffective due to cracks and spalling in the coating.

FOREWORD

This report was prepared by the University of Dayton Research Institute under Air Force Contract No. F33615-95-D-5029, Delivery Order No. 0003. The work was administered under the direction of the Nonmetallic Materials Division, Materials Directorate, Wright Laboratory, Air Force Materiel Command, with Dr. James R. McCoy (WL/MLBC) as Project Engineer.

This report was submitted in June 1997 and covers work conducted from 14 September 1995 through 28 April 1997.

SECTION 1
THE EFFECT OF ISOTHERMAL AGING ON THE STRUCTURE AND PROPERTIES OF AFR700B

1.1 INTRODUCTION

A variety of environmental factors, acting individually or synergistically, can have a profound influence on the performance of advanced polymers and composites. The current trend in the aerospace industry is toward lighter weight materials with improved high-temperature properties. As a result, fiber-reinforced polymeric composites are being applied in structures which are exposed to elevated service temperatures in excess of 300°C. These high-temperature exposures often occur after or in conjunction with, exposure to humid environments. The combined effects of these environments can lead to an alteration of the physical and chemical structure of the resins as well as the fibers and fiber-resin interfaces. These changes can, in turn, result in a decline in the mechanical properties of the composite material.

Polyimides are a class of polymer which contain an imide linkage. Aromatic polyimides have been developed for use in high-temperature applications because of their relatively high glass transition temperatures and high thermal oxidative stability. The presence of rigid aromatic and polyimide heterocyclic units imparts high stiffness and thermal stability to the polymer backbone. The type and density of crosslink reactions can further enhance the resin modulus and thermal oxidative stability.

Polymerization of monomer reactants (PMR) polyimides were developed in the early 1970's by Serafini and coworkers [1]. These addition-type polyimides exhibited the easy processing and high use temperature characteristics required of advanced composites. PMR polyimide materials are the product of the reaction of three different monomers: a diamine, a

diester-diacid, and an ester-acid end cap. These reactions are usually conducted in a solution of methanol.

The most widely used PMR resin is PMR-15. The processing steps of PMR-15 are shown in Figure 1. The general reaction scheme is similar for other addition-type polyimides with the exception of differing monomeric reactants, differing polymer molecular weights, and some differences in the end group chemistry associated with crosslinking. The PMR approach to processing of polyimides allows for easier processing than would ordinarily be possible with these largely insoluble polymers.

The PMR approach can be used for polymer formation from monomer reactants directly on graphite fibers during composite processing. Two major steps have been identified during the cure reaction. The first step yields a polyimide prepolymer and occurs in the temperature range of 100-250°C, the second step occurs above 275°C and involves the reaction of the norbornene end caps and gives rise to the crosslinked structure [2].

The proposed imidization reaction scheme involves the conversion of the aromatic diester diacid to a dianhydride and then subsequent reaction of that unit with the diamine to form an imide link [2,3]. Spectroscopic evidence of an anhydride intermediate during the imidization reaction led to the proposition of the reaction schemes in Figure 2. The reaction pathway labeled A involves the formation of a dianhydride from the diester diacid. The reaction pathway labeled B involves the reversion of the polyamic acid to yield the anhydride groups. Infrared spectroscopy data suggest the reaction scheme A is the actual reaction pathway to the imidization reaction [2,3].

Monomeric Reactants:

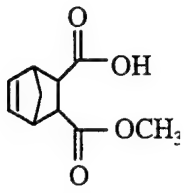

NE
2.000 moles

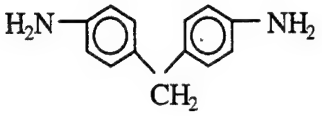

MDA
3.087 moles

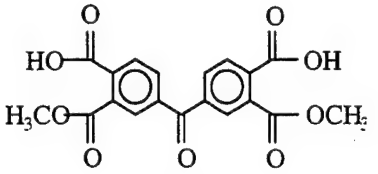

BTDE
2.087 moles

Room Temperature to 150°C

Amide acid prepolymer:

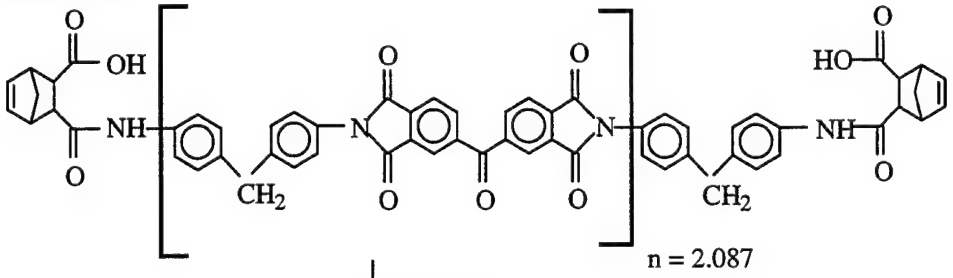

n = 2.087

150-250°C

Imidized prepolymer:

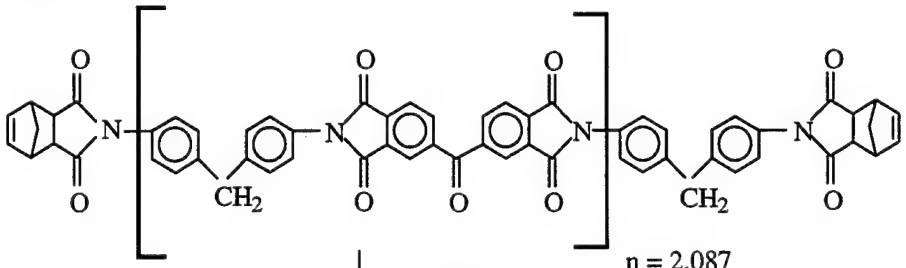

n = 2.087

250-316°C Under Pressure

Thermally crosslinked polyimide:

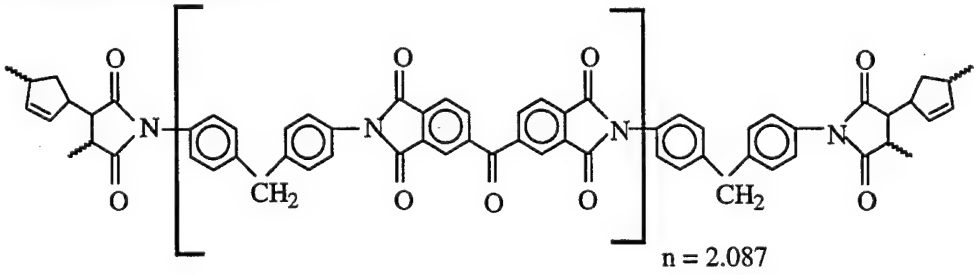

n = 2.087

Figure 1. General Reaction Scheme for Cure of PMR-15.

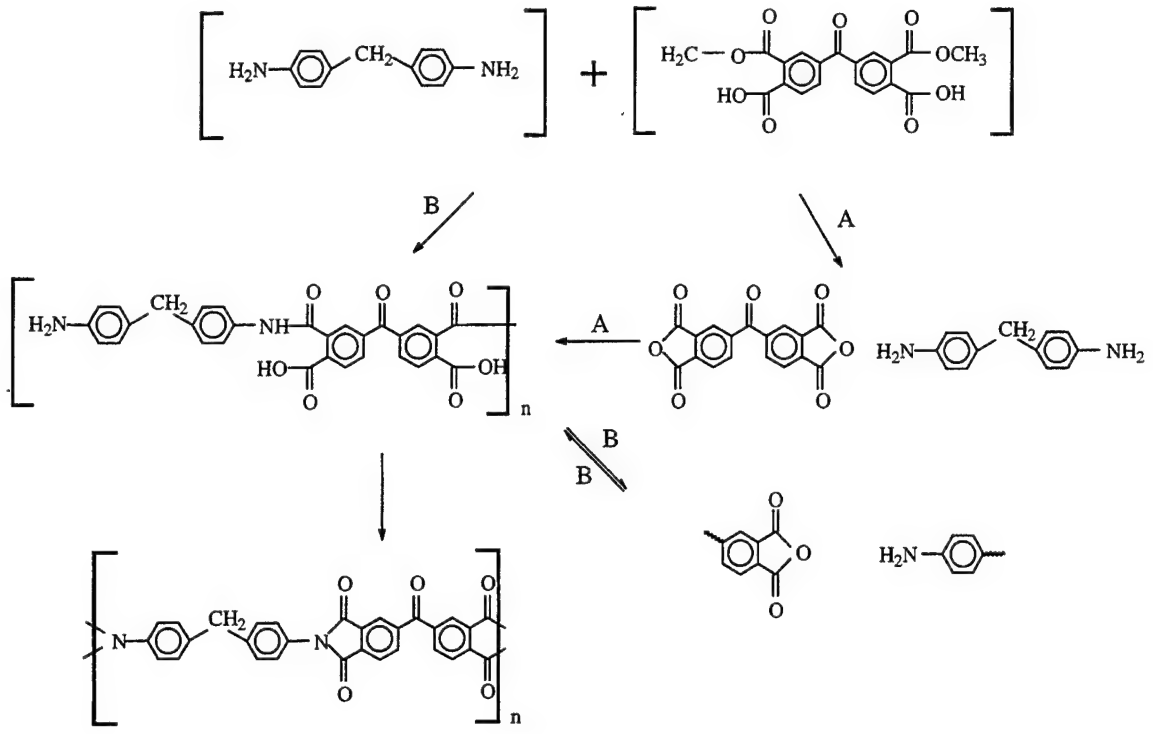

Figure 2. Imidization Reaction Scheme.

The reaction of the norbornene group has been omitted from Figure 2. It has been shown that the monomethyl ester acid of 5-norbornene-2,3-dicarboxylic acid reacts with the amine to form an imide very quickly at room temperature [3]. As a result, any anhydride formation of the end group would not be detectable in the infrared spectroscopy due to its high reactivity [2].

After formation of the imidized prepolymer, subsequent processing involves isomerization of the nadic end-capped oligomer (Figure 3) and a retro Diels-Alder reaction (Figure 4) [4]. The isomerization of the endo-isomer to the exo-isomer occurs in the addition-type polyimides in the temperature range of 175 to 260°C, simultaneous to the imidization reaction.

(a) Exo-end cap (b) Endo-end cap

Figure 3. Isomerization of the Nadic End Cap.

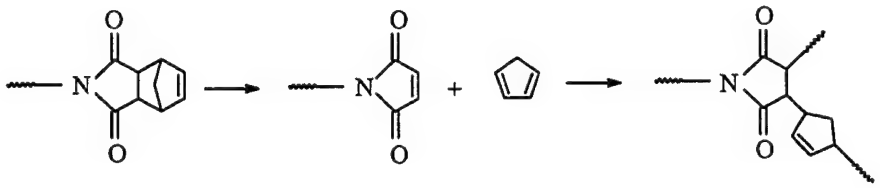

Figure 4. Proposed Retro Diels-Alder Crosslinking Reaction for Norbornene End-Groups.

Polyimides with norbornene end groups are believed to crosslink through a retro Diels-Alder reaction (Figure 4). The retro Diels-Alder reaction of the norbornene end groups results in the formation of a maleimide group and cyclopentadiene. These two units then recombine and undergo a thermally-induced free-radical polymerization reaction to form a crosslinked structure containing cyclopentene crosslinks [4]. A variety of crosslink structures are possible with and without the cyclopentene. In addition the cyclopentadiene can react with norbornene units to form doubly-bridged adducts. Some of the possible crosslink structures are shown in Figure 5 [4].

Some common aerospace polyimides are shown in Figure 6. The differences in molecular weight, backbone chemistry, and crosslink reactions alter the final thermal and mechanical properties of each of these polymers.

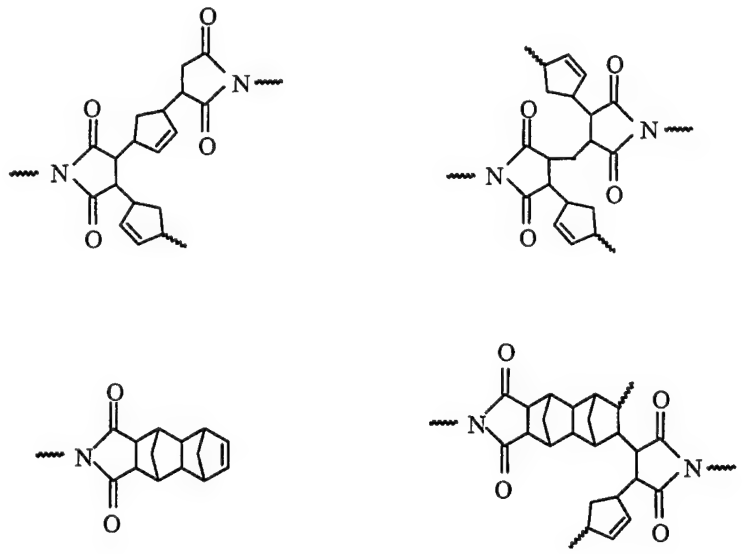

Figure 5. Some Possible Crosslink Structures Resulting from Retro Diels-Alder Reactions.

(a) PMR-15

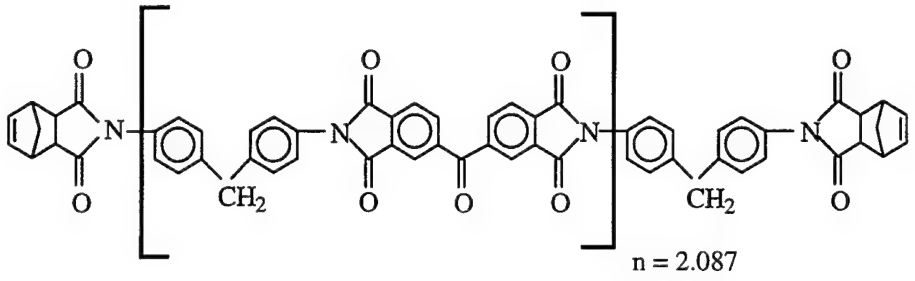

(b) PMR-II-50

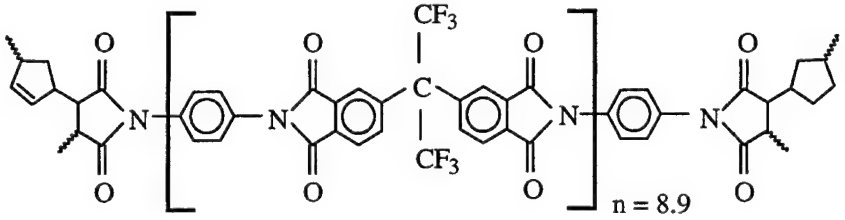

(c) AFR700B

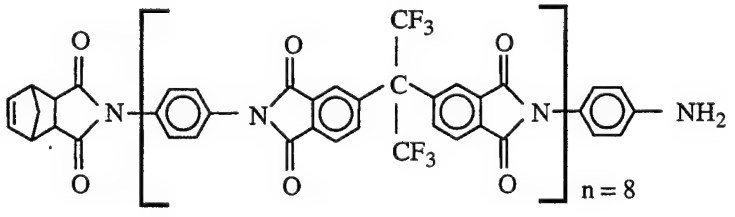

Figure 6. Some Aerospace-Grade Polyimides.

AFR700B is formulated with a scarcity of end cap such that it is only singly terminated with a norbornene end group. As a result it is believed to undergo a Michael addition reaction during crosslinking (Figure 7). This reaction is a common curing reaction for bismaleimide (BMI) resins cured with diamines. BMIs can be cured using diamines to extend the polymer chains which results in both increased network flexibility and fracture toughness.

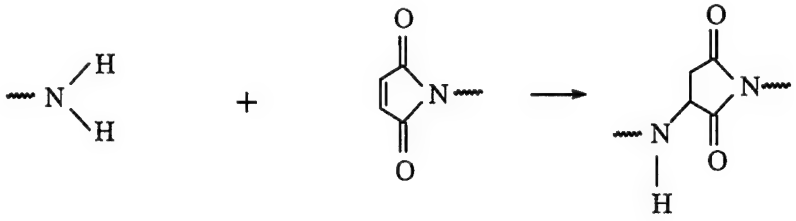

Figure 7. Michael Addition Reaction.

In AFR700B the Michael addition reaction can occur after the formation of cyclopentadiene and a maleimide group during the retro Diels-Alder reaction. The maleimide may react with an amine and result in the formation of a Michael addition crosslink. As a result of this reaction, excess cyclopentadiene may be present in the material. This product may react elsewhere in the structure or may be evolved. Inadequate reaction or removal of the cyclopentadiene can result in porous final structures.

In addition to the Michael addition reaction, BMI resins can undergo homocrosslinking (Figure 8). A similar reaction can occur during the retro Diels-Alder reaction in many of the PMR-type polyimides. These reactions can also result in the formation of excess cyclopentadiene which must be further reacted or removed for the formation of quality laminates.

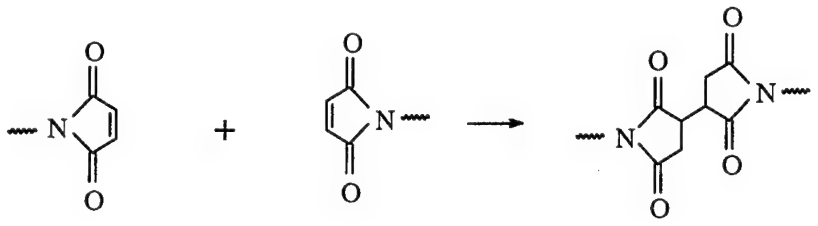

Figure 8. Homocrosslink.

These polyimide resins can also undergo a thermooxidative crosslinking process to form carbon-oxygen ether linkages between polymer backbones. This is believed to occur through the reaction of existing carbonyl groups or carbonyl groups which are formed after scission of some of the trifluoromethyl ($-CF_3$) groups from polymers such as AFR700B.

The critical steps in the processing of polyimides involve the removal of reaction by-products such as water and alcohol from the imidization reaction as well as other low molecular weight by-products such as unreacted cyclopentadiene [5]. If these reaction by-products are not adequately removed, fabricated panels will be porous. This porosity can lead to a lowering in mechanical performance and accelerated degradation due to enhanced diffusion of moisture and oxygen.

The addition polyimides can have a variety of imide linkages. Some imide linkages are associated with the polymer backbone, while other imide and succinimide linkages are associated with the end-group reactions which occur during crosslinking. It is the crosslinking reactions which provide these materials with exceptional thermal stability [4]. Hydrolytic degradation can occur through hydrolysis of any of the imide linkages. The effect of that degradation on the mechanical and thermal performance of the system is dependent upon the relative extent of degradation of each type of imide linkage. Evidence exists for hydrolytic degradation of both types of imides in AFR700B [6].

Recently, degradation of polyimide resins has been reported as a result of hygrothermal exposure [7,8]. Under these conditions the glass transition temperature (T_g) decreases with exposure time. This decrease has been attributed to physical [7] and chemical [6,9] changes occurring in the resin.

The origin of physical aging is shown in Figure 9. During processing, the material is cooled from an elevated temperature to the use temperature. During cooling, the free volume of the material decreases continually. Once the specimen temperature reaches the glass transition temperature of the material, lack of molecular motion inhibits the ability of the material to continue to alter its conformation, and the rate of free volume decrease changes considerably. Over time, as a specimen is aged at a temperature below its glass transition temperature, the free volume will decrease and approach the equilibrium free volume condition. This process is called physical aging.

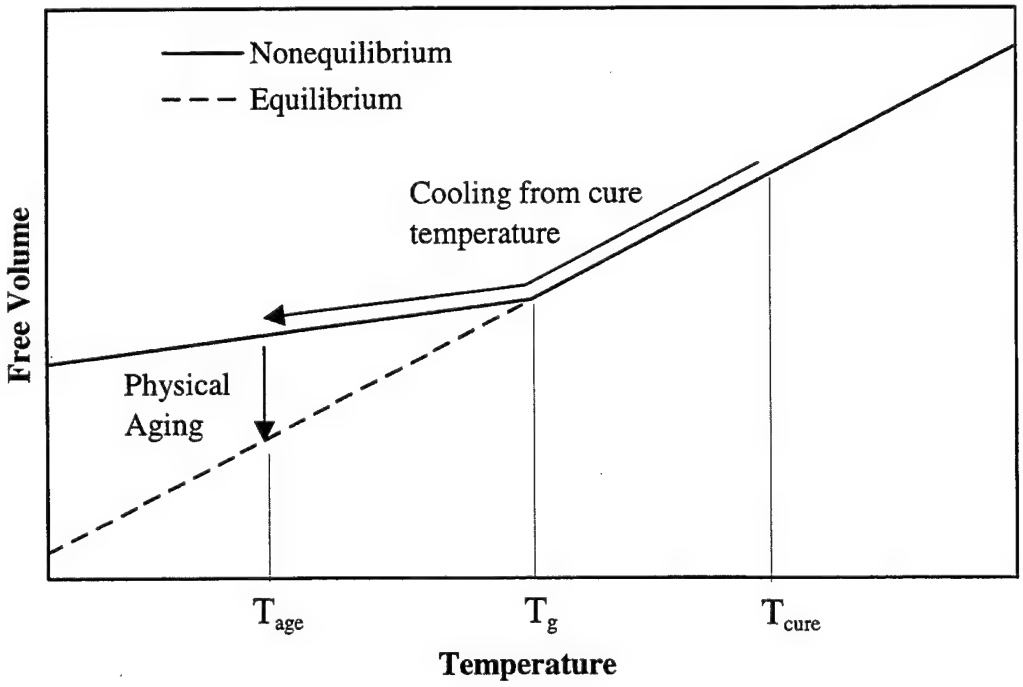

Figure 9. The Origin of Physical Aging.

During processing polymeric materials can undergo physical alterations in the polymer conformation. In the rubbery or liquid states, molecular motions of polymers can involve 10 to 50 carbon atoms. However, in the glassy state molecular motions are restricted to vibrations, rotations, and motions of relatively short chain segments. The molecular motion of longer chain molecules is hindered, and the polymer chains are typically in a nonequilibrium conformation when in the glassy state. As a result the molecules in the structure undergo a slow process to rearrange into a lower energy conformation. Such molecular motions are termed physical aging and can lead to an alteration of the mechanical and physical properties of the material.

The nonequilibrium glassy state is unstable, and the polymer undergoes slow processes to approach equilibrium. Physical aging is the gradual process which is actually a continuation of the glass formation process that was initiated near the T_g. As a result physical aging affects all the temperature-dependent properties which change at or near the T_g of the material [10].

Physical aging generally occurs during isothermal exposures or during slow cooling from an elevated temperature. However, it can also occur during thermal cycling and should be considered during treatments which include long-term exposures.

As a result of physical aging, a small but measurable increase in the rigidity of the resin occurs with time. Changes in shear modulus of the polymer can be used as a measure of the effect of physical aging on the material. The changes in modulus occur primarily at temperatures near the aging temperature, T_a, and decrease in magnitude with decreasing T_a [11]. Material property changes associated with physical aging are reversible if the material is exposed to a temperature at or above T_a.

During long-term aging at an elevated temperature, a sample may also undergo additional crosslinking. This can result in an increase in T_g and an increase in the rubbery modulus of the specimen. Each of these effects can be observed in the dynamic mechanical spectra of a specimen.

Many polymers undergo chemical changes when exposed to humid environments, particularly at elevated temperatures. Polyimides have been shown to undergo hydrolysis under such conditions [9,12]. The hydrolysis reaction is a simple reversal of the imidization reaction which occurred during cure of the polymer (Figure 10) [13]. Nuclear magnetic resonance studies have shown that polyimides differ in their susceptibility to hydrolytic degradation. Variations in backbone structure and steric hindrance can greatly affect the hygrothermal stability of these polyimide resins [9]. The exact nature of the chemical changes which these polyimides undergo in service environments is an area which requires further study. In addition the effects of these chemical changes on mechanical and physical properties are still unclear.

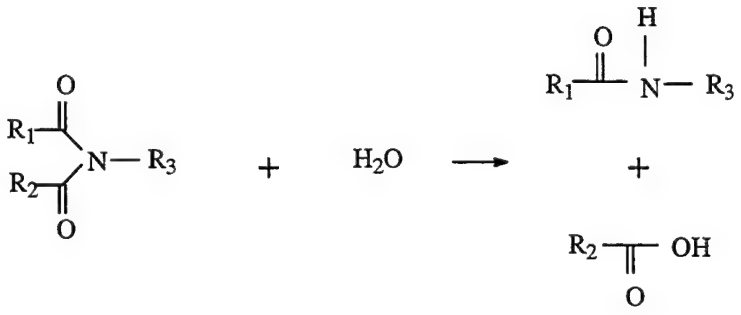

Figure 10. Imide Hydrolysis.

1.2 EXPERIMENTAL

1.2.1 Materials and Sample Preparation

Studies were conducted on a neat polyimide resin, AFR700B, derived from a mixture of nadic ester, paraphenylenediamine (PPDA), and dimethyl 4,4'-(hexafluoroisopropylidene)-bis(phthalate) (6FDA), and obtained from Daychem, Inc. as a 70 weight percent solution in methanol. The structure of the AFR700B resin is shown in Figure 11. Neat resin plates of AFR700B, 2.3 mm thick, were processed in a hot press which produced a T_g of approximately 360°C in the as-cured state. Some of these plates were further postcured in a nitrogen atmosphere to give a T_g of approximately 430°C. These resin plates were then cut into rectangular specimens, measuring 4.5 cm x 0.6 cm, which were dried to a constant weight in a vacuum oven at 50°C.

1.2.2 Environmental Exposure

Specimens were placed in three glass cloth-lined steel bags. A gas inlet port was then positioned at the base of each bag. These bags were placed in an oven maintained at 250°C, and continuous streams of dry air, humid air, or nitrogen gas were allowed to flow through them. The sources of the inlet gas streams were (1) compressed air filtered through a desiccant, (2) compressed air percolated through a heated water bath, and (3) liquid nitrogen. The gas flow through each port was maintained at approximately 62 cc/minute throughout the experiment. The bags were initially purged with the respective gases, and the flow was then adjusted to maintain a slight positive pressure in each bag. After 500 and 1000 hours at 250°C, specimens were removed, weighed, and dried to constant weight in a vacuum oven at 50°C. All specimens were stored under these conditions until testing.

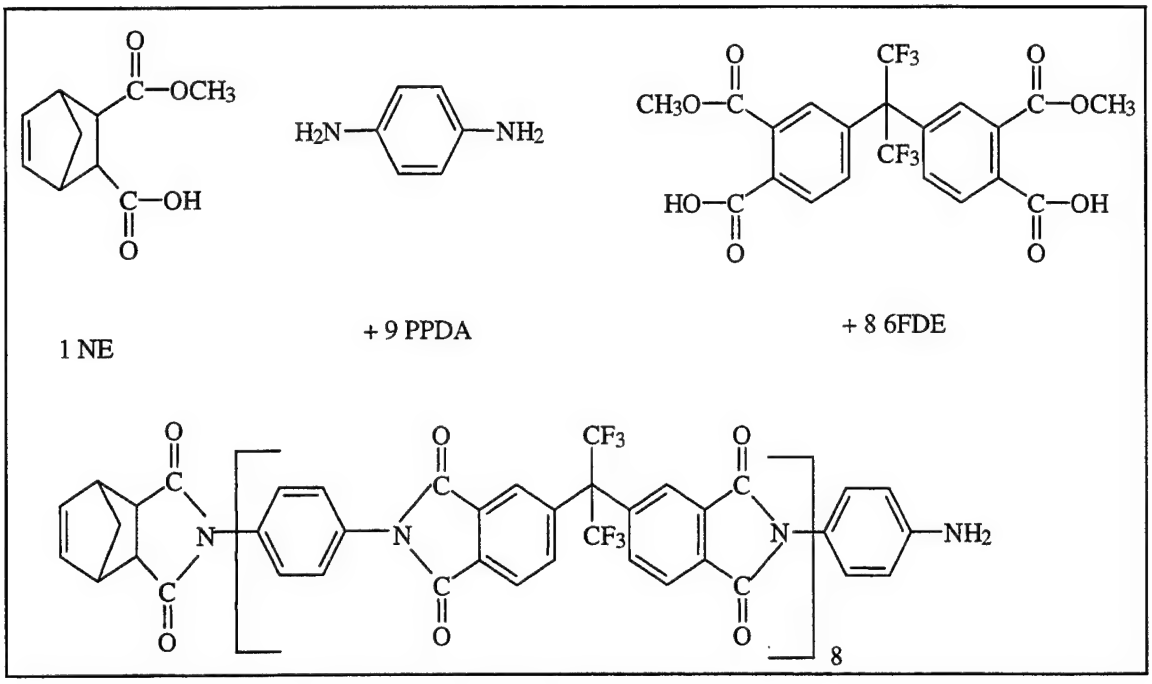

Figure 11. Formulation for AFR700B Resin.

1.2.3 Property Evaluation

Specimens were tested in a Rheometrics dynamic mechanical analyzer operating in the torsion mode. Temperature scans were conducted at 100 radians/second and a heating rate of 2°C/minute to determine the T_g of specimens. All reported glass transition temperatures are the average of two specimens and were determined from the maximum in the loss modulus (G") peak. Frequency sweeps were conducted from 0.1 to 100 radians/second, between 50°C and 490°C, at temperature intervals of 20°C. Time-temperature superposition was used to generate a master curve for each specimen. The relaxation spectra were generated from master curves of the storage modulus using the method of Tschoegl, as described by Ferry [14].

1.3 DATA ANALYSIS

A first approximation of the relaxation spectrum was first generated using

$$H(\tau) = dG'/d \ln \omega + (1/2)\, d^2G'/d(\ln \omega)^2 \qquad (1)$$

where $1/\omega = (2)^{1/2}\, \tau$. When the slope of this curve is negative, the alternate equation

$$H(\tau) = dG'/d \ln \omega - (1/2)\, d^2G'/d(\ln \omega)^2 \qquad (2)$$

where $1/\omega = \tau /(2)^{1/2}$, was used. Calculation of the terms $dG'/d \ln \omega$ and $d^2G'/d(\ln \omega)^2$ in the above equations requires smoothing of the experimental data prior to numeric differentiation. In some practical problems, interpolation of a single polynomial is not a suitable approximation of a function or data set; to obtain a good approximation by an *n-th* degree polynomial, it may be necessary to use a large value of *n*. Unfortunately, polynomials of a large degree often have highly oscillatory behavior which is not desirable in approximating functions or data that are reasonably smooth. To overcome the oscillatory behavior of polynomials and still provide a smooth approximation, the use of cubic splines has proven quite effective. In this technique, instead of approximating the whole data range with a single spline, several basic cubic spline functions, defined in segments of the data range, are used.

Consider an interval $a \leq x \leq b$ over which a function $f(x)$ is to be approximated with spline functions. A set of spline functions defined in subdivisions $[a=x^{(1)}<x^{(2)}<x^{(3)}<...<x^{(m)}=b]$ of the interval yield a better approximation than the use of one spline function for the whole interval (see Figure 12).

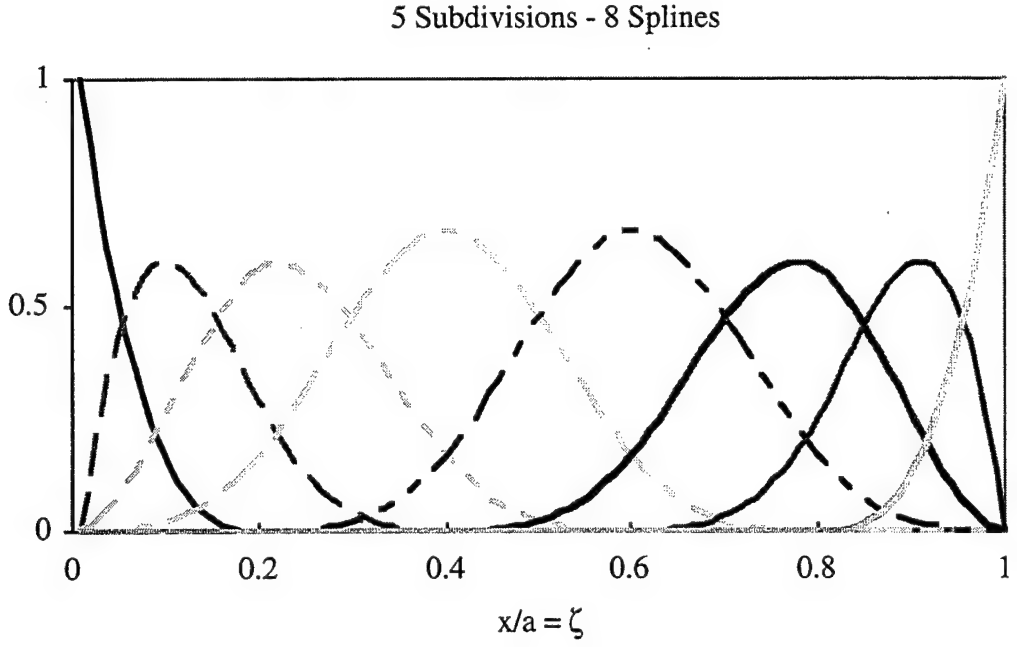

Figure 12. Example of Multiple Splines.

The spline functions $X_{n,i}(x)$ used were developed by Iarve [15] using the following recursive procedure:

$$X_{n+1,i}(x) = \frac{I_{n,i-1}(x)}{I_{n,i-1}(x_m)} - \frac{I_{n,i}(x)}{I_{n,i}(x_m)}, \quad i = 2,\ldots,n+m; \tag{3}$$

$$X_{n+1,1}(x) = 1 - \frac{I_{n,1}(x)}{I_{n,1}(x_m)}, \quad X_{n+1,n+1+m}(x) = \frac{I_{n,n+m}(x)}{I_{n,n+m}(x_m)}, \tag{4}$$

where

$$I_{n,i}(x) = \int_a^x X_{n,i}(\xi)d\xi$$

$$X_{0,i}(x) = 1, x_i \le x \le x_{i-1} \text{ and } X_{0,i}(x) = 0,\ x_{i-1} > x, x > x_i,\ i = 1,\ldots,m.$$

The subscript n used in the notation of the spline function, $X_{n,i}(x)$, indicates the order of the spline. For cubic spline functions, n is equal to 3. Using these cubic splines as the basis, the approximated function for $f(x)$ is defined as

$$F(x) = \sum_{1}^{m+3} C_i X_{3,i} \tag{5}$$

where C_i are arbitrary constant coefficients. For m subdivisions in the interval $[a=x^{(1)}<x^{(2)}<x^{(3)}<...<x^{(m)}=b]$, the number of cubic spline functions defined in the interval is $m+3$. If the function $f(x)$ is known at p distinct points $(x_1, x_2, ..., x_p)$, then $f(x)$ is best approximated by minimizing the error in the least square sense

$$\varepsilon = \sum_{1}^{p} [f(x_i) - F(x_i)]^2 \tag{6}$$

The coefficients C_i in Equation 5 are determined by minimizing the error ε by setting $\frac{d\varepsilon}{dC_i} = 0$. This leads to a set of systems of equations which can be solved for C_i [16]:

$$A^T A C = A^T f \tag{7}$$

where

$$A = \begin{bmatrix} X_{3,1}(x_1) & X_{3,2}(x_1) & \dots & X_{3,m+3}(x_1) \\ X_{3,1}(x_2) & X_{3,2}(x_2) & \dots & X_{3,m+3}(x_2) \\ \dots & \dots & \dots & \dots \\ X_{3,1}(x_p) & X_{3,2}(x_p) & \dots & X_{3,m+3}(x_p) \end{bmatrix}$$

$$C = \begin{bmatrix} C_1 & C_2 & \dots & C_p \end{bmatrix}^T$$

$$f = \begin{bmatrix} f(x_1) & f(x_2) & \dots & f(x_p) \end{bmatrix}^T$$

and A^T is the transposed matrix of A. Equation 7 is an (m+3) x (m+3) linear system of equations, and the coefficients C_i are determined by solving numerically, using the LU decomposition technique in this case [17]. The determination of C_i thus yields the best-fitted curve in the least square sense, as given by Equation 5. This spline variational technique provided excellent

agreement between the experimental and approximated data. This allowed smoothing of the experimental data and subsequent numeric differentiation.

1.4 RESULTS AND DISCUSSION

1.4.1 Exposure Conditions

The experimental conditions were not strictly controlled in regards to the content of moisture in the gas streams. The amount of moisture in the humid air was significantly greater than the amount of moisture in either of the other gas streams. However, the nitrogen and "dry" air gas streams did contain a trace amount of moisture. The elevated temperature at which the aging was conducted prohibited direct measurement of the relative humidity in each environment. Room temperature measurements of humidity were conducted to estimate the amount of moisture present in each gas stream. The "dry" air had a relative humidity of 19 percent at 23°C, the humid air had a relative humidity of 100 percent at 25°C, and the nitrogen had a relative humidity of 19 percent at 22°C. Each of these conditions is equivalent to a relative humidity at 250°C of less than one percent. However, the humidified air had five times more moisture than either of the other gas streams, which translates to a significantly higher amount of water vapor flowing over the specimens at 250°C.

Material property changes after aging in nitrogen should reflect the influence of physical aging and continued chemical reaction. Comparison of the results from specimens aged in dry air and nitrogen should allow an estimate of the added influence of thermal oxidation, and comparison of results from specimens aged in dry and humid air should provide insight into the influence of moisture-induced degradation (such as hydrolysis) on material properties.

1.4.2 Effect of Aging on Glass Transition Temperature

The initial T_g of the as-cured specimens was approximately 360°C. The T_g of all these specimens increased significantly after aging at 250°C. The specimens aged in humid air displayed a smaller increase than the specimens aged in dry air or nitrogen (Figure 13). The initial T_g of the postcured specimens was approximately 430°C. After 500 hours at 250°C the T_g of the specimens exposed to dry air and nitrogen remained relatively unchanged. However, the specimens aged in humid air showed a decline in T_g of approximately 15°C (Figure 14). After 1000 hours at 250°C, the T_g of the dry air-aged specimen declined by about 15°C, while the specimens exposed to humid air showed a T_g decline of about 30°C.

The increase in the T_g of as-cured specimens suggests additional crosslinking occurring during aging. The smaller increase in humid air, compared to dry air or nitrogen, could be due to an inhibition of the crosslinking by the moisture present or, more likely, due to competition between crosslinking and concurrent chemical degradation in the hygrothermal environment. This conclusion appears to be corroborated by trends observed in the thermomechanical spectra (Section 1.4.3). The postcured specimens did not experience an increase in T_g as a result of aging at 250°C. The T_g of specimens aged in nitrogen remained relatively unchanged, while the T_g of specimens aged in humid air declined by as much as 30°C after 1000 hours at 250°C. This decline is significant and suggests a breakdown in the polymer structure as a result of the moisture exposure. The exact nature of this chemical breakdown was not addressed in this study. However, the fact that it occurred in the presence of moisture, while specimens aged similarly in nitrogen experienced no change (as reflected by the measured T_g), suggests hydrolysis. The slight decline in T_g after aging for 1000 hours in dry air may be a result

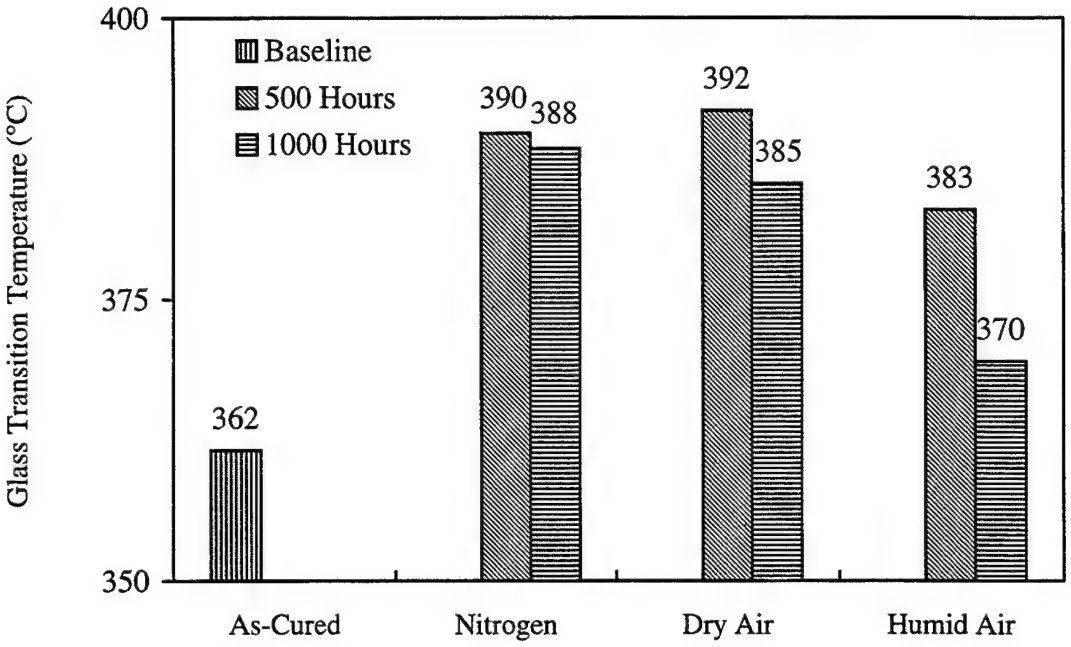

Figure 13. Glass Transition Temperature as a Function of Aging Environment for As-Cured Specimens.

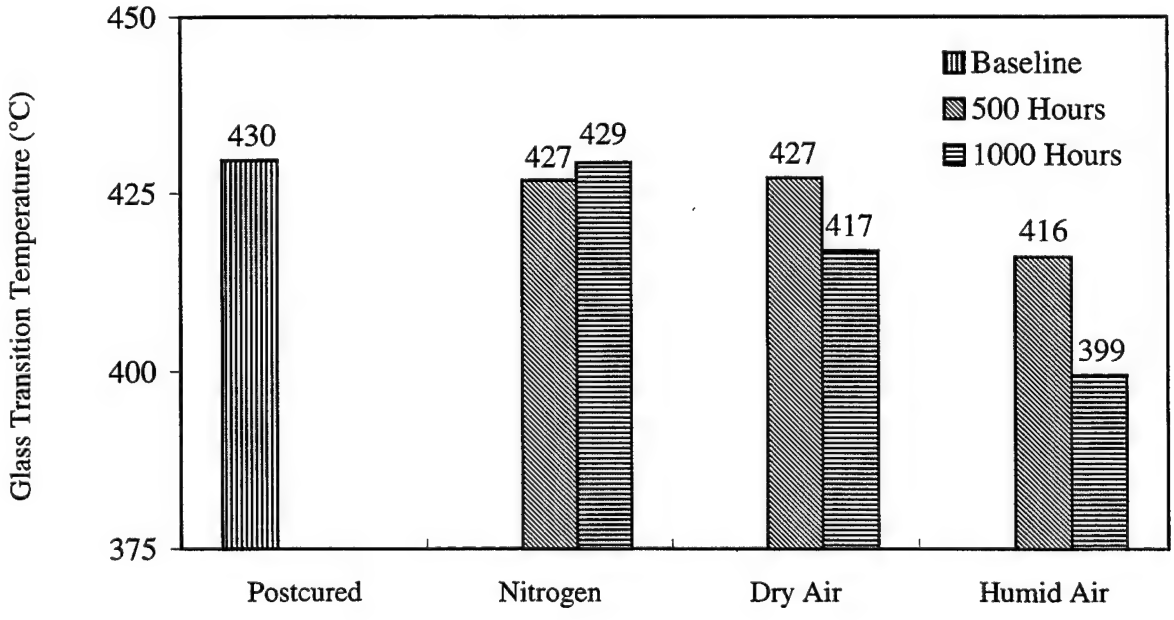

Figure 14. Glass Transition Temperature as a Function of Aging Environment for Postcured Specimens.

of a small amount of moisture which was measured in the "dry" air flow or could suggest an oxidative component to the degradation.

1.4.3 Effect of Aging on Thermomechanical Spectra

The thermomechanical spectra used to determine the glass transition temperature revealed additional information about the effect of aging on the molecular structure of the resin. For the as-cured specimens, the shape of the storage modulus (G') curve in the thermomechanical temperature sweep changed after aging; the aged specimens displayed appreciably larger dynamic shear modulus above T_g than the baseline specimen. Due to the susceptibility of these resins to additional crosslinking when exposed to temperatures above the T_g, a true rubbery modulus cannot be directly obtained from this data. However, from the data in Figure 15, the trend above the T_g is apparent; the baseline specimen has the lowest modulus in this region followed by the specimen aged in humid air, while the curves for specimens aged in dry air and nitrogen overlap at higher modulus values. This trend is similar to that observed in T_g measurements (Figure 13) and may reflect additional crosslinking during aging. The baseline postcured specimen (not shown), as expected, has a modulus substantially higher than any of the (unaged or aged) as-cured specimens due to its higher degree of crosslinking.

For ideal rubbers a relative crosslink density can be calculated from the modulus in the rubbery plateau region by using Equation 8 [18]

$$n = \frac{G_r}{RT} \tag{8}$$

where n is the relative crosslink density, G_r is the apparent modulus in the rubbery region, R is the ideal gas constant, and T is the absolute temperature. The highly crosslinked nature of AFR700B and the lack of a true rubbery modulus make direct application of this technique

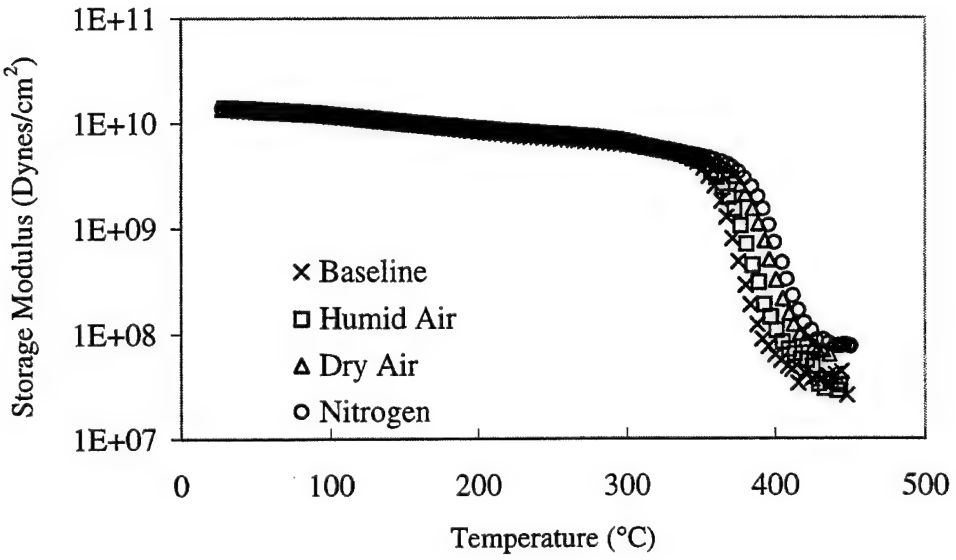

Figure 15. Storage Modulus as a Function of Temperature for the As-Cured Specimens that were Aged for 1000 hours.

invalid. However, a relative value can be determined and used to compare the effect of various environments on the crosslink density. For the purposes of comparison, an arbitrary crosslink density of 0.0 was assigned to the value calculated for the as-cured specimens, and 1.0 was assigned to the value calculated for the postcured specimens. All other specimens were normalized according to these two values, and the results are presented in Figures 16 and 17. These results suggest that the as-cured specimens undergo additional crosslinking when exposed to 250°C environments. In humid air this effect is diminished, most likely as a result of a competing degradation process. The postcured specimens showed some evidence of additional crosslinking in nitrogen, but the primary operating mechanism was the degradation process which occurred in the humid environment.

The relationship between relative crosslink density and glass transition temperature is shown in Figure 18. The as-cured specimens primarily experienced an increase in both T_g and crosslink density as a result of aging at 250°C, regardless of the aging environment.

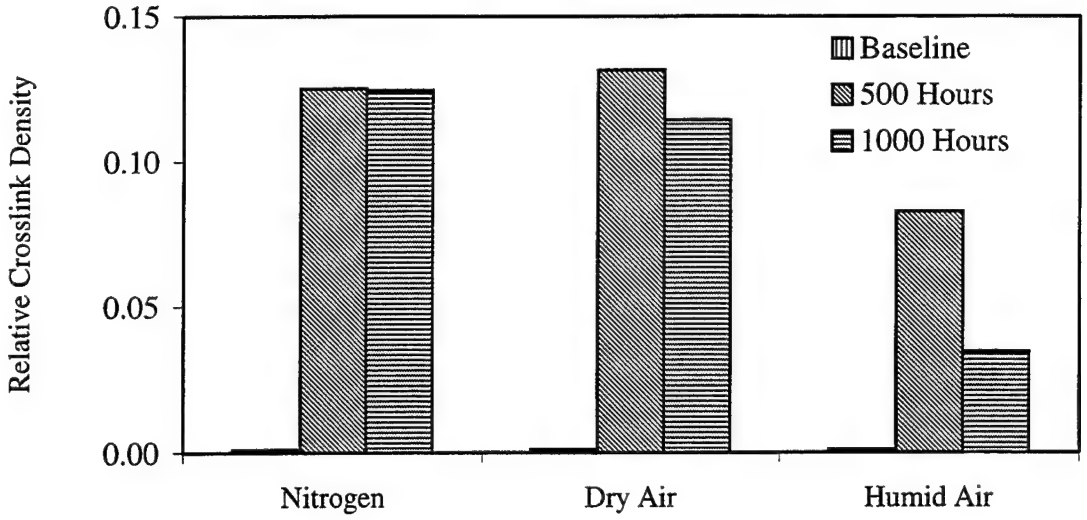

Figure 16. Relative Crosslink Density for As-Cured Specimens.

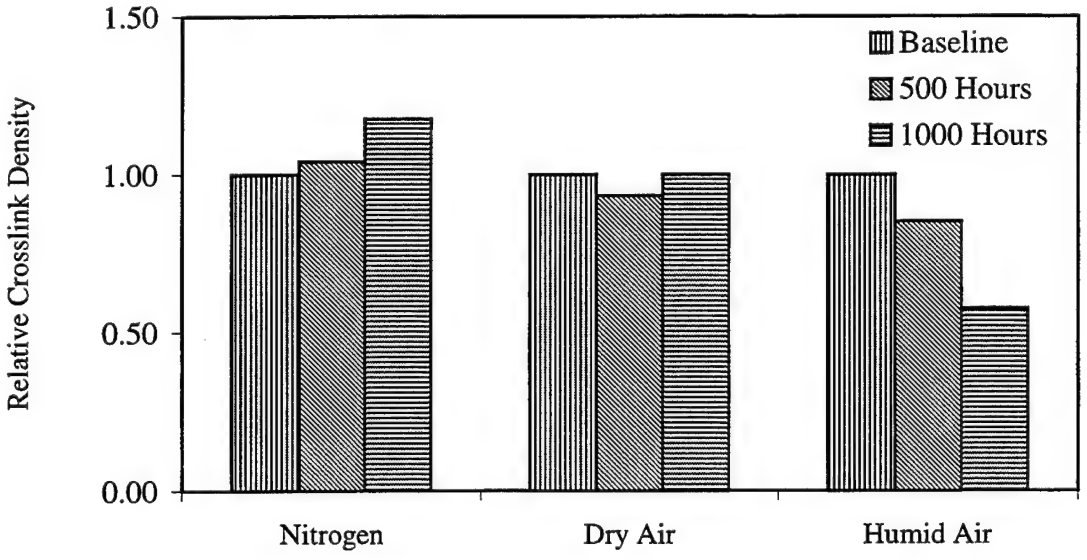

Figure 17. Relative Crosslink Density for Postcured Specimens.

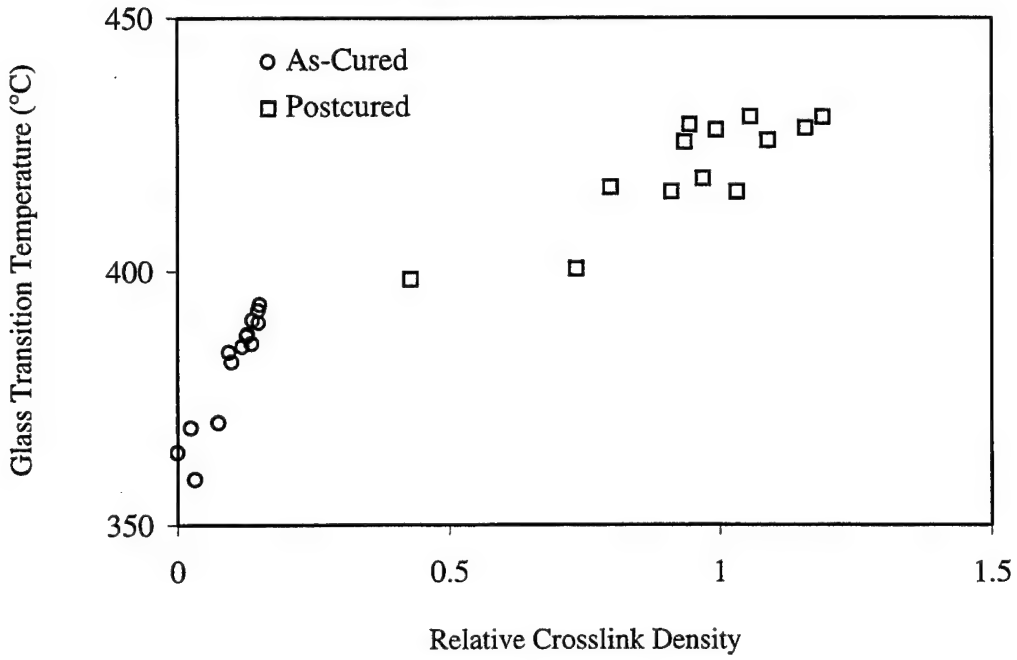

Figure 18. Glass Transition Temperature as a Function of Relative Crosslink Density.

The extent of increase in T_g and crosslink density was dependent upon the relative humidity of the aging environment. The postcured specimens primarily experienced a decrease in both T_g and relative crosslink density as a result of aging, with the extent of that decrease being dependent upon the relative humidity of the aging environment.

The storage modulus generated from temperature sweeps of unaged and aged postcured specimens are shown in Figure 19. In the vicinity of the aging temperature (250°C), there is an expected increase in modulus for all aging environments. This increase is attributed to physical aging. This effect disappears as the temperature scan exceeds the aging temperature.

Regardless of the aging environment or the initial cure state, the shape of the α-peak in the G" and Tan δ curves was altered after aging. In each case a shoulder appeared on this curve in the region below the T_g (Figure 20) suggesting the occurrence of additional molecular motions in this temperature range. A change in T_g with aging resulted in a lateral shift

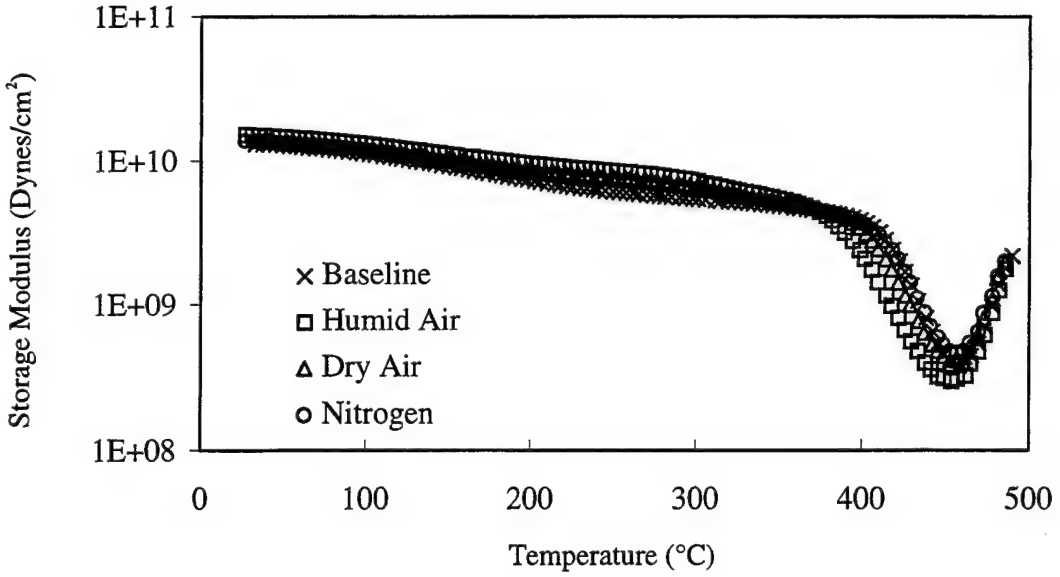

Figure 19. Storage Modulus of Postcured Specimens Aged for 1000 hours.

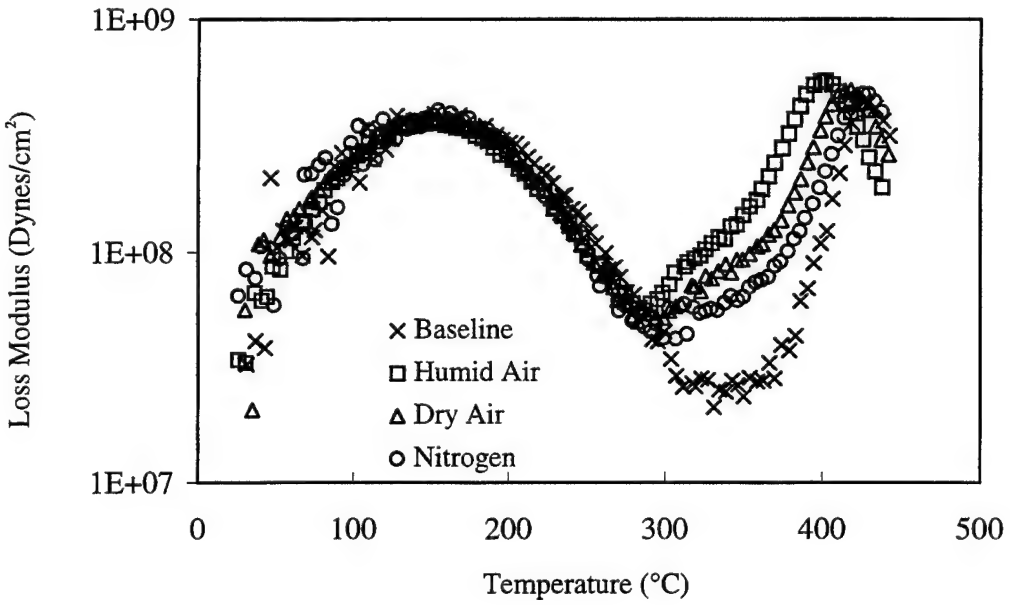

Figure 20. Loss Modulus of Postcured Specimens Aged for 1000 hours.

of this shoulder along with the α-peak but with no change in shape or intensity. Similar shoulders have previously been attributed to stresses frozen into polymers as a result of processing or quenching [19,20].

1.4.4 Effect of Aging Environment on Relaxation Spectra

The relaxation spectra, $H(\tau)$, provides additional insight into the physical and chemical alterations which have occurred in a polymer as a result of environmental exposure. Figure 21 shows the relaxation spectra for unaged and aged postcured specimens. The initial peak corresponds to ß-transitions in the resin occurring deep in the glassy state. Physical aging is not expected to alter the ß-transition because the amount of molecular motions possible at those temperatures and/or frequencies is generally considered too small to be measurable [10]. As expected, therefore, the ß-transition in Figure 21 showed no changes for all the aging conditions from the short-time edge through the peak. The long-time edge of the ß-transition for the aged specimens showed a decrease in $H(\tau)$ compared to the baseline specimen. A corresponding increase in the $H(\tau)$ over the baseline value was observed at the short-time edge of the α-transition for all the aged specimens. The area between the curves for the baseline and aged specimens in the short-time region of the α-transition is similar to the area between the same curves in the long-time region of the ß-transition. These results suggest that physical aging caused a shift in the relaxation times toward longer times, independent of the aging environment. The equivalence of these shifts suggests that the rates and mechanisms of physical aging are the same in all the aging environments. The specimens which were aged in humid air showed a small additional increase in $H(\tau)$ on the short-time edge of the α-transition, over the baseline specimens as well as those aged in nitrogen and dry air. This suggests the generation of

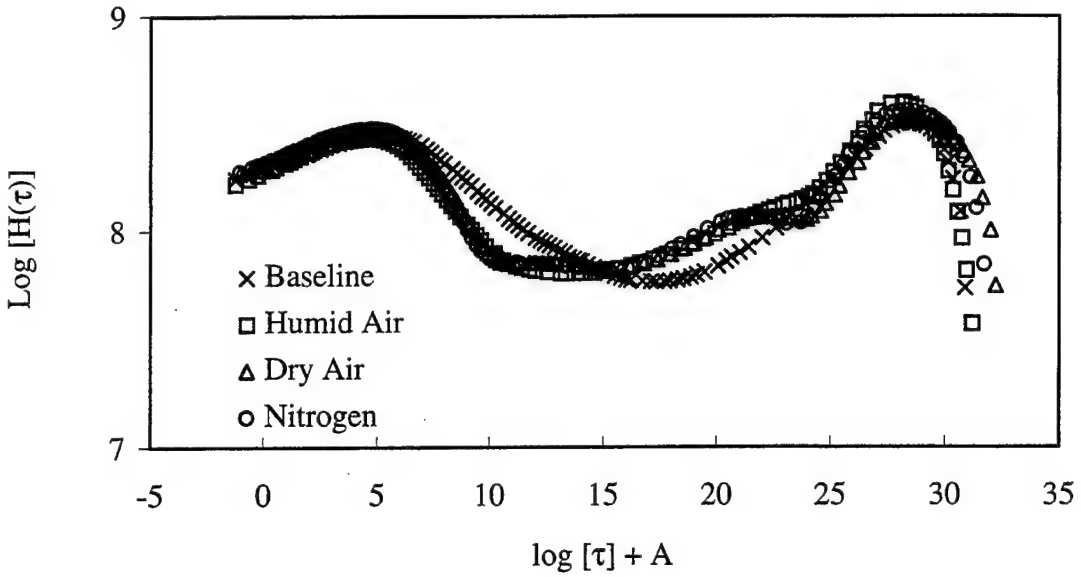

Figure 21. Relaxation Spectra of Postcured Specimens Unaged and After Aging for 1000 hours.

additional relaxation processes which were not present after exposure to the other aging conditions.

1.4.5 Effect of Aging Environment on Thermooxidative Degradation

Prior to the aging experiment each specimen was initially dried to constant weight in a vacuum oven at 50°C. The weight of each specimen was then monitored throughout the exposure period. Some weight loss is expected in the air environments as a result of thermooxidative degradation. Figure 22 shows the extent of weight loss for an average of about eight specimens under each aging condition. The error bars represent one standard deviation for each mean. Some weight loss is apparent under each aging condition. The weight loss associated with the nitrogen-aged specimens is most likely a result of evolution of absorbed moisture which was not removed during the low-temperature vacuum oven exposure. At the elevated temperature of the exposure, however, the diffusivity of moisture is greater, and some

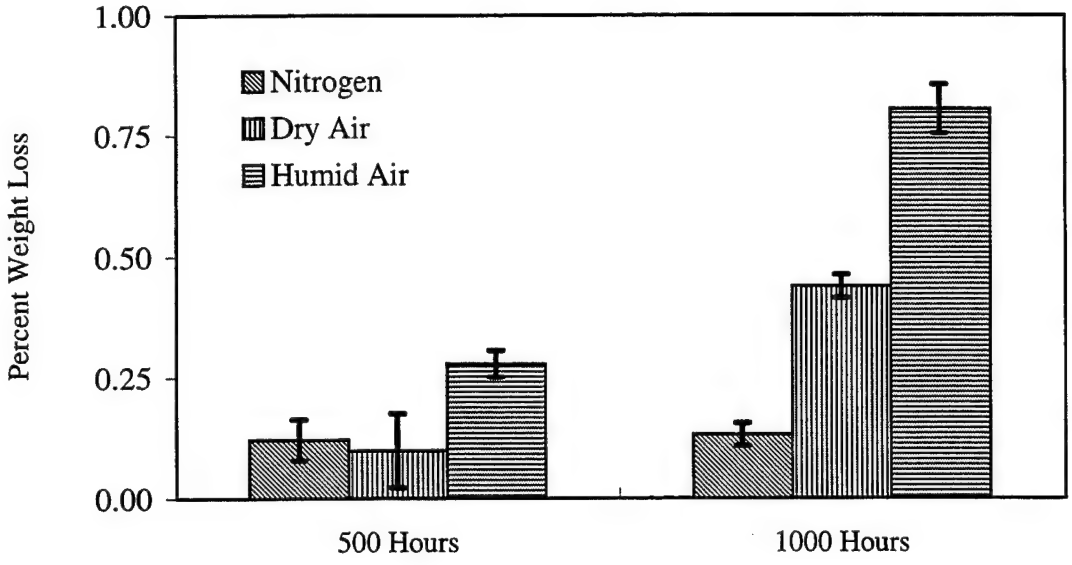

Figure 22. Percent Weight Loss of Specimens After Aging.

residual moisture would be expected to diffuse out of the specimen, particularly during the long exposure times of this experiment. The specimen weight data shows that this moisture appears to be removed within the first 500 hours of exposure, and the specimen weights do not change appreciably after that point. Due to the relatively low concentration of oxygen in the nitrogen gas stream environment, these specimens are not expected to undergo an appreciable amount of thermooxidative degradation.

Of course, the amount of oxygen in the two air streams was significantly greater, and thermooxidative degradation is expected to occur at these test temperatures. The specimens aged in dry air exhibited a measurable amount of weight loss which was probably a result of thermooxidative degradation and residual moisture. The specimens aged in moisture air appear to be particularly sensitive to thermooxidative degradation, displaying measurable weight loss after just 500 hours and substantial degradation after 1000 hours. These results suggest that moisture has enhanced the chemical degradation process, possibly through hydrolysis and

subsequent volatilization of low molecular weight species, or through enhanced thermooxidative degradation.

1.5 SUMMARY AND CONCLUSIONS

Neat as-cured and postcured AFR700B polyimide resin was aged for 1000 hours at 250°C in dry air, humidified air, and dry nitrogen. Thermomechanical and relaxation spectra data suggest that physical aging occurred in all the aged specimens in a similar manner, regardless of the aging environment. Increases in glass transition temperature and apparent rubbery storage modulus of the as-cured specimens provided evidence of additional crosslinking as a result of aging. The magnitude of these changes was reduced in the specimens aged in humid air, probably due to the competing influence of moisture-induced chemical breakdown of the molecular structure. The decline in the glass transition temperature of postcured specimens, and the appearance of additional features in the relaxation spectra of specimens aged in humid air, support the suggestion of molecular breakdown under prolonged hygrothermal exposure. Weight loss of the specimens suggests that the presence of moisture in the aging environment can enhance the thermooxidative degradation process.

SECTION 2
HYDROLYTIC EXPOSURE OF AFR700B

A research program was initiated to develop a fundamental understanding of the mechanisms leading to hydrolytic degradation in high-temperature organic matrix composites. Studies were performed on neat resin specimens to limit the number of variables associated with the degradation processes. An accelerated test was developed to simulate the environment that resin is exposed to during rapid heating when the specimen moisture content and temperature are high. This test procedure decreases the exposure time and resources required during previous research activities which involved multiple transfers of specimens between a humidity chamber and an oven [7,21].

2.1 ACCELERATED HYDROLYTIC CONDITIONING

A controlled characterization method for evaluating the susceptibility of various high-temperature resin systems to hygrothermal degradation is required. Because hydrolytic degradation is a function of the material moisture content, it is important to limit moisture diffusion and drying while the sample is maintained at an elevated temperature. The method is intended to simulate the worst-case condition during operation, which is maximum moisture content at elevated temperatures. During accelerated hygrothermal conditioning, neat resin samples are first saturated in a humidity cabinet (85 percent RH/29.5°C) and then placed in sealed stainless-steel hydraulic tubing which has been filled with a sufficient quantity of distilled water to ensure that the sample will be exposed to saturated steam at the desired test temperature. The samples are placed on top of a packing to ensure that they are not immersed in liquid. The saturated steam surrounding the specimen will prevent drying and thus preserve a uniform

moisture content. The sample weight is measured "dry" prior to exposure, "wet" after exposure in the humidity cabinet and after exposure to steam, and finally after redrying in a vacuum oven at 110°C. Ideally a mass balance could then be used to determine the degree of hydrolysis as will be discussed later.

2.2 GLASS TRANSITION TEMPERATURE MEASUREMENT

The glass transition temperature (T_g) of each specimen was measured under dynamic torsion by a Rheometrics RDS-II. Samples were vacuum dried to constant weight at 110°C prior to testing. The strain rate was 100 rad/sec, the strain was 0.1 percent, and the heating rate was 10°C/minute. In most cases two samples were measured per condition. The T_g was defined as the peak maximum of the loss modulus, G".

2.3 NEAT RESIN TENSILE PROPERTIES MEASUREMENT

Tensile properties of neat resin were measured on 15 x 1.27-cm, straight-sided specimens using an Instron 5582 test machine. Testing was conducted on hydrolytically-aged specimens which were vacuum dried at 110°C. A clam shell oven was used to heat the samples for testing at 250°C and 300°C. A special extender fixture was developed to permit strain measurement of the sample with a conventional clip-on extensometer placed outside the clam shell oven. Multizone temperature control of the oven was used to ensure that the test temperature was highest at the 2.5-cm gage section. The Instron crosshead displacement was 1.27 mm/minute.

2.4 EFFECT OF HYDROLYTIC EXPOSURE ON T_g

AFR700B neat resin samples were aged in saturated steam at 100°C, 125°C, 150°C, 175°C, and 200°C. The resultant dry T_g of the conditioned specimens is shown in Figure 23.

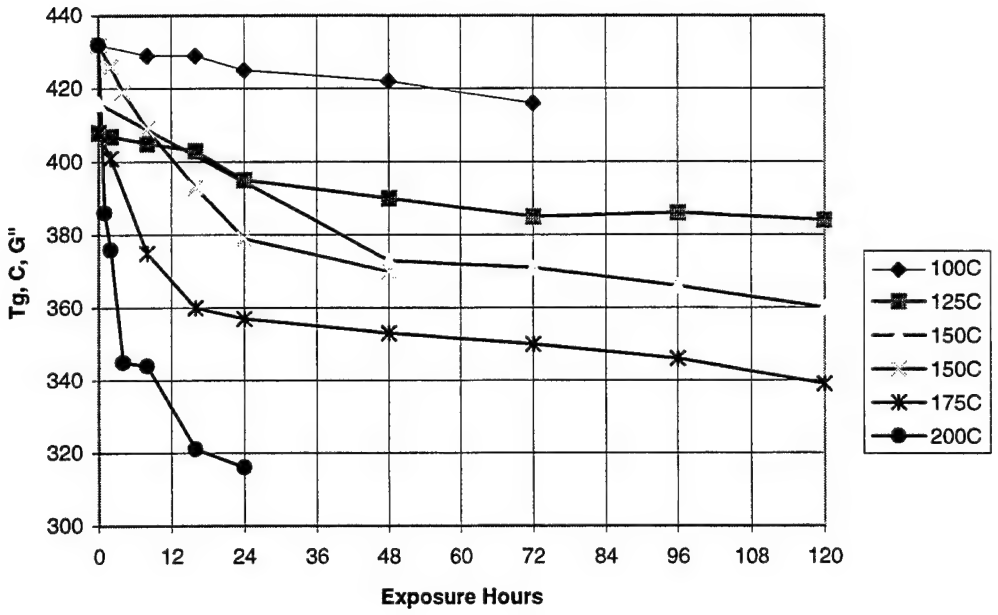

Figure 23. Dry T_g of AFR700B Samples After Accelerated Hydrolytic Conditioning.

After 16 hours of exposure at 200°C, 150°C, and 100°C, the T_g decline was 110°C, 40°C and 4°C, respectively. Perhaps the most surprising result was that a reduction in T_g of 16°C occurred after 72 hours of aging at 100°C. This indicates that attempts to dry thick parts at a "low" temperature prior to use can still lead to property reduction, although at a much slower rate than typical operating temperatures.

During the accelerated procedure the moisture content of the resin increased slightly from 4.2 percent (after aging in the humidity cabinet) to 4.8 percent (after exposure to saturated steam). As previously stated the goal of the accelerated hydrolytic conditioning is to simulate the worse-case condition when moisture content and temperature are at their highest. There is little reason to believe that the accelerated test results in unrealistic chemical degradation; however, prolonged exposure at 200°C did result in unexpected damage. Figure 24 shows the "redried" resin weight change after the exposure to saturated steam. During the first eight hours of

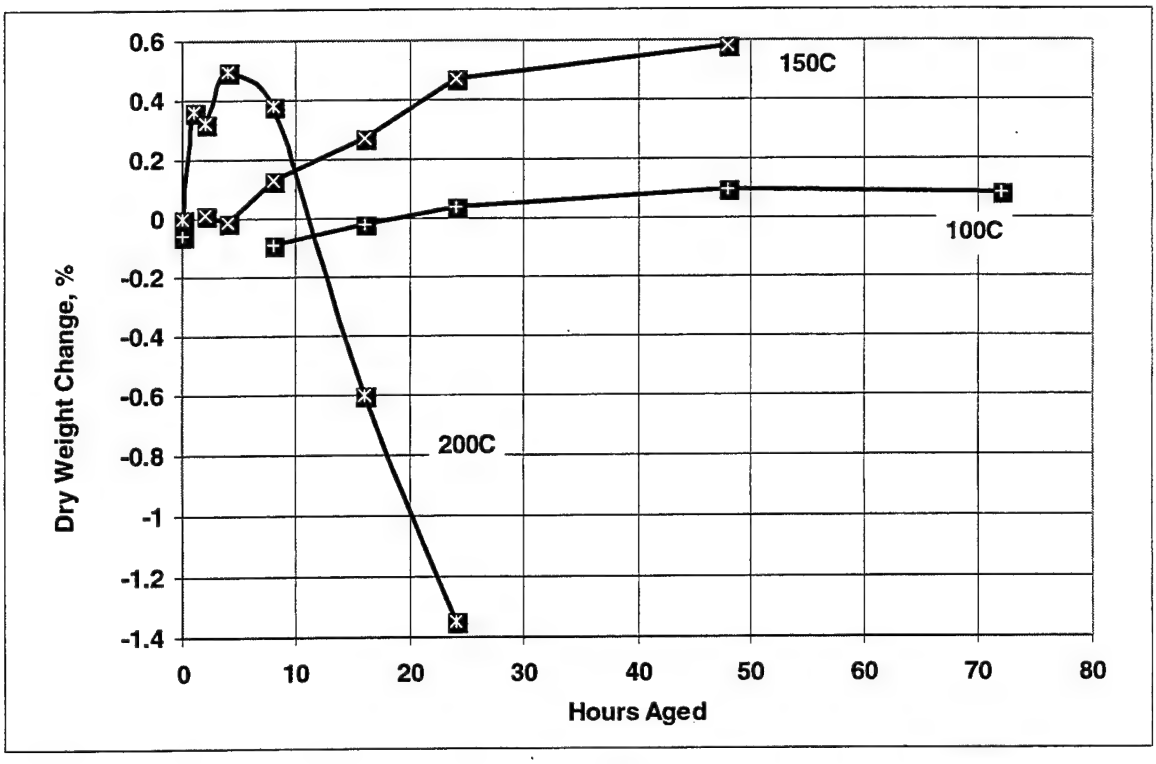

Figure 24. Weight Change of Vacuum-Dried AFR700B Samples After Steam Exposure.

exposure at 200°C, there was a weight increase followed by a steep weight loss. This resulted from the extraction of low molecular weight components from the hydrolytically-degraded resin which were readily observed through a discoloration of the distilled water used in the pressure vessel. Samples aged at 150°C and 100°C showed only an increase in dry weight after aging, and no discoloration of the distilled water was observed. Following this observation it was decided that long-term exposures at 200°C were too severe, and a standard exposure temperature of 150°C was selected.

It is believed that the dry weight gain after aging results from chemically-bound water in the resin. NMR studies conducted by Curliss [6] indicated that hydrolysis of imide linkages is occurring. Theoretically, an increase in weight of 0.4 percent would result in an average of one hydrolyzed imide linkage per chain out of a possible 17 (AFR700B MW=4400, H_2O MW=18).

Forty-eight hours of aging in saturated steam at 150°C resulted in a dry weight increase of 0.58 percent and a decline in T_g of 63°C. The fact that a relatively small percentage of possible sites are readily hydrolyzed indicates that specific sites may be more vulnerable. It is also interesting to note that TGA-mass spectroscopy data taken during the postcure of as-cured AFR700B indicate that water does evolve. These data suggest that imide linkages formed during the postcure may be highly strained and thus more vulnerable to hydrolysis.

The reduction in T_g is reversible when the resin is heated to its typical postcure temperature of 400°C. A torsion specimen with a T_g of 370°C after aging for 48 hours at 150°C in saturated steam was aged isothermally at 400°C for six hours. The T_g of the postcured specimen nearly returned to its original value of 432°C. A similar study was conducted with an isothermal hold at 300°C to determine if it is likely that an AFR700B composite part would recover its T_g in service. After a prolonged hold of 66 hours at 300°C in nitrogen, the sample T_g increased only slightly from 365°C to 370°C. Although the chemical hydrolytic degradation is reversible, it is unlikely to occur within an operational environment.

The effect of oxidation on hydrolytic stability was also investigated. AFR700B neat resin specimens were aged for 100 hours at 371°C and then exposed to saturated steam at 150°C. Figure 25 provides a comparison of the dynamic storage modulus of the four conditions: (1) unaged, (2) oxidized, (3) oxidized followed by 48-hour steam exposure, and (4) 48-hour steam exposure only. The data show that the oxidized sample does not have a well-defined T_g; in addition only a mild transition is apparent after steam exposure. These data suggest that oxidative crosslinking enhances the hydrolytic stability of AFR700B. However, during a transient process, oxidation should occur to a greater extent near the surface of a specimen, and

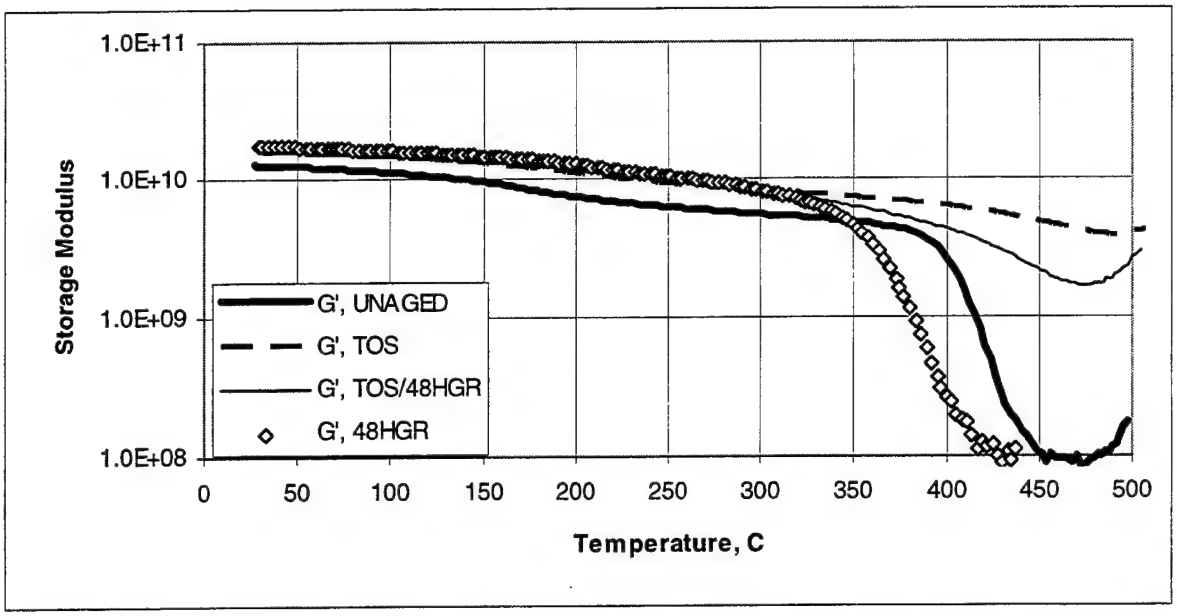

Figure 25. DMA Data of Environmental Effects on Storage Modulus, G', for AFR700B.

hydrolysis should occur to a greater extent toward the specimen center. This will result in no real benefit to oxidative crosslinking with regard to hydrolytic stability enhancement.

2.5 AFR700B TENSILE PROPERTIES

The AFR700B neat resin tensile samples had a postcured T_g of 432°C which was reduced to 384°C and 368°C after aging at 150°C in saturated steam for 24 and 48 hours, respectively. The tensile properties shown in Figures 26 and 27 were evaluated at 250°C and 300°C. The ultimate stress at 250°C was reduced 38 percent after 48 hours of exposure, while a 49 percent reduction occurred at a test temperature of 300°C. The secant modulus at 250°C remained unchanged after 48 hours of exposure, while a 43 percent reduction occurred at a test temperature of 300°C. This is a surprising reduction in properties considering that the specimen T_g was 368°C. Figures 28 and 29 show representative stress-strain curves before and after aging. The sample yielding observed in the stress-strain curve resulted from necking in the gage section.

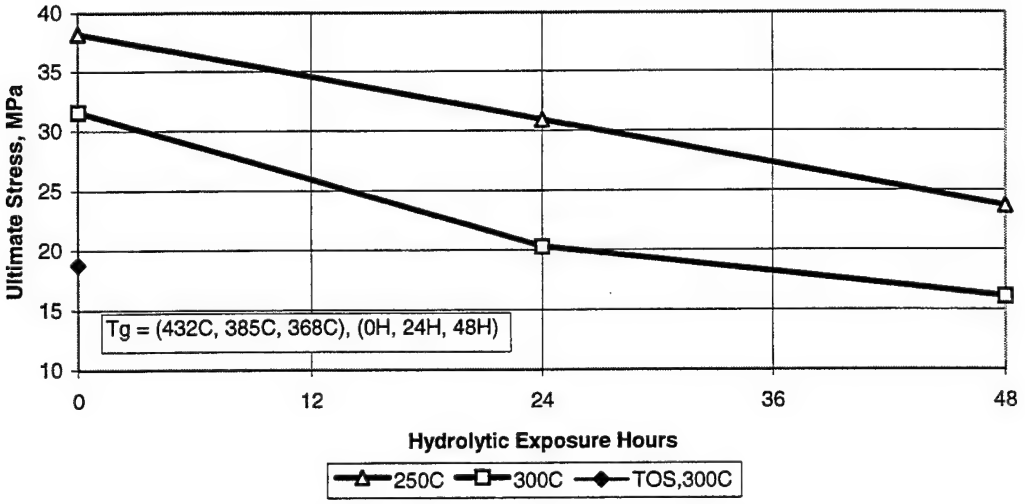

Figure 26. Ultimate Tensile Stress of AFR700B Resin after Exposure.

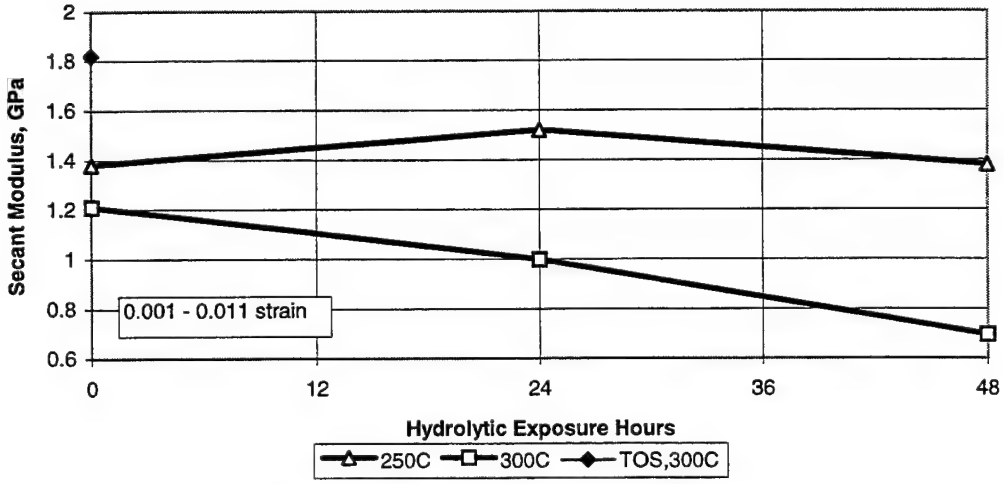

Figure 27. Secant Tensile Modulus of AFR700B Resin after Exposure.

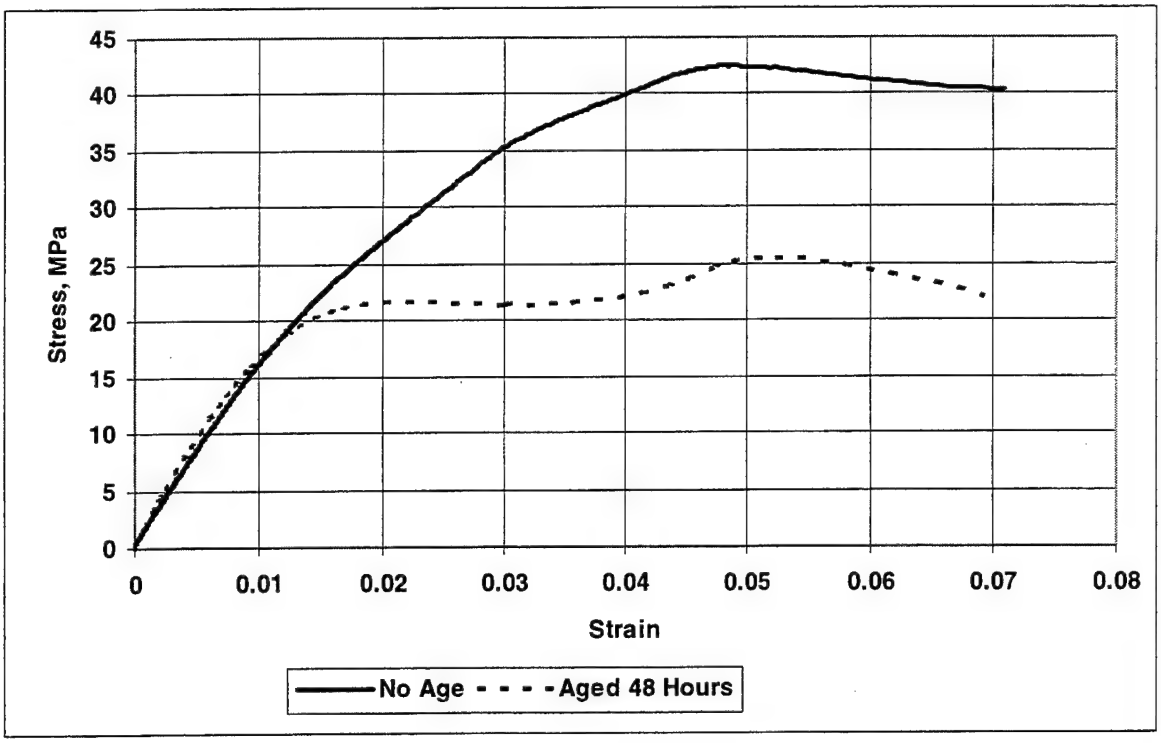

Figure 28. Stress-Strain Curves, at 250°C, of AFR700B Tension Samples after Exposure to Saturated Steam at 150°C.

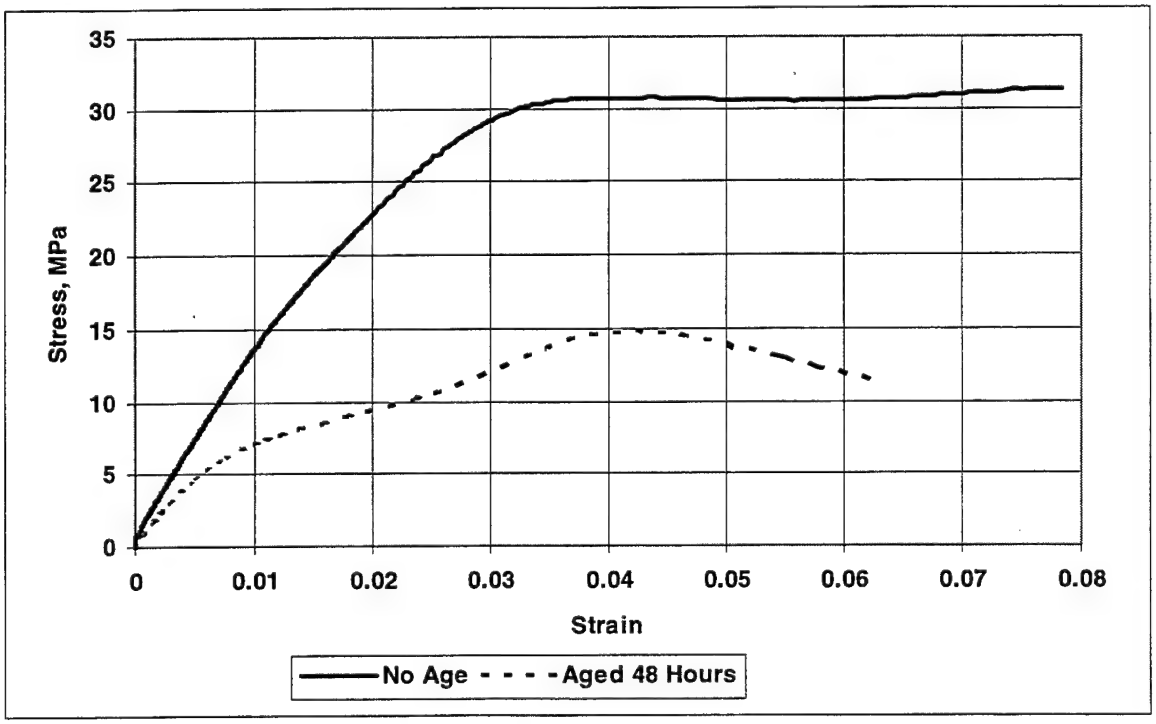

Figure 29. Stress-Strain Curves, at 300°C, of AFR700B Tension Samples after Exposure to Saturated Steam at 150°C.

SECTION 3
MOISTURE DIFFUSION IN AFR700B

A series of desorption (drying) experiments under isothermal conditions were performed in a Cahn microbalance. Data suggest that the Fickian diffusion model is valid up to the point of sample blistering. From these diffusivity data, shown in Figure 30, an Arrhenius expression for the temperature-dependent diffusivity has been determined to be

$$D = 0.0652 \exp\left(\frac{-4118}{T}\right)$$

where the mass diffusivity, D, is in cm^2/s and the temperature, T, in Kelvin.

A one-dimensional model for temperature and moisture concentration distributions was constructed to predict the moisture content for a flat panel undergoing a temperature cycle. Although for the thickest (0.16") sample at the highest heating rates (up to 50°C/min before reaching isothermal condition in the Cahn balance, or when heated at 20°C/min ramp), up to a 15-degree temperature differential could exist in the sample. Inclusion of heat transfer did not always improve the accuracy of the model. The model was therefore simplified by eliminating the temperature distribution computations. The predictive capability is verified by comparing the predicted to the measured moisture content during drying. A typical set of results is shown in Figure 31. Of the 11 isothermal cases the maximum error is 0.07 (fraction of saturation). Of the four cases where drying was under various constant temperature ramp rates, shown in Figure 32, the maximum error is slightly higher at about 0.1.

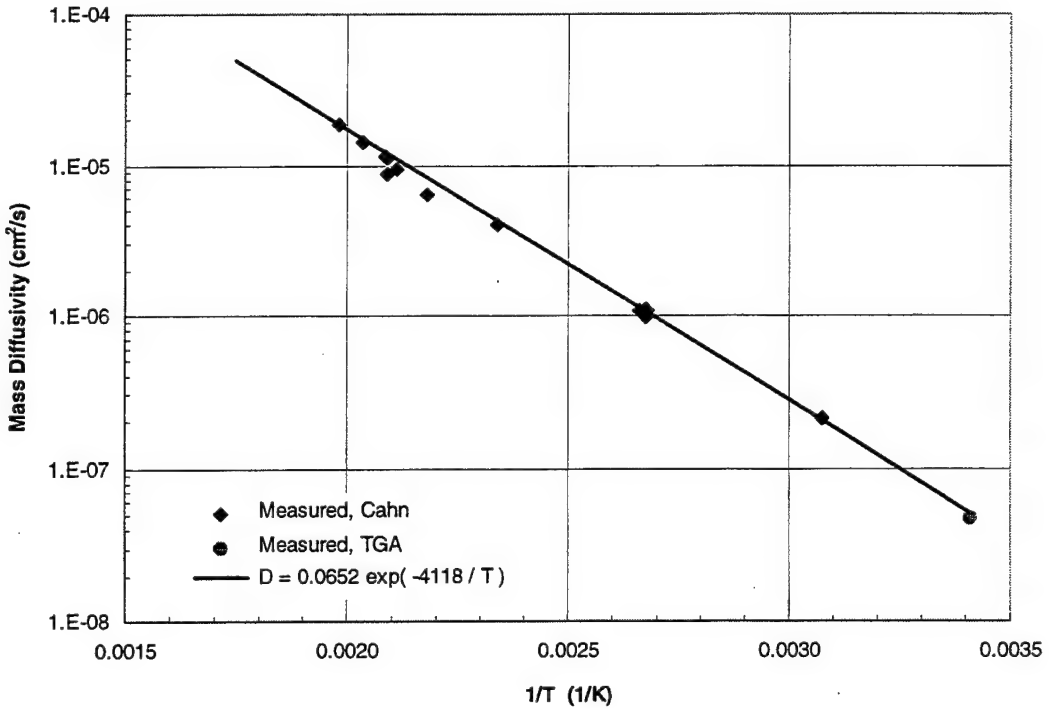

Figure 30. Mass Diffusivity of Water in AFR700B at Various Temperatures.

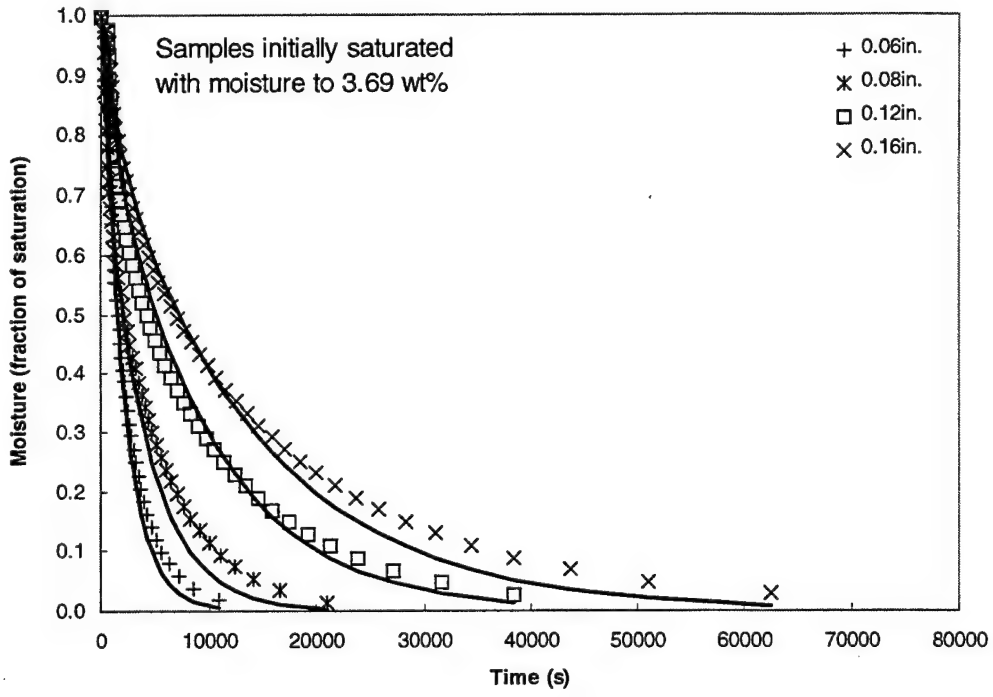

Figure 31. Measured (markers) and Predicted (curves) Moisture Content in Samples of Different Thicknesses Undergoing Isothermal Drying at 100°C.

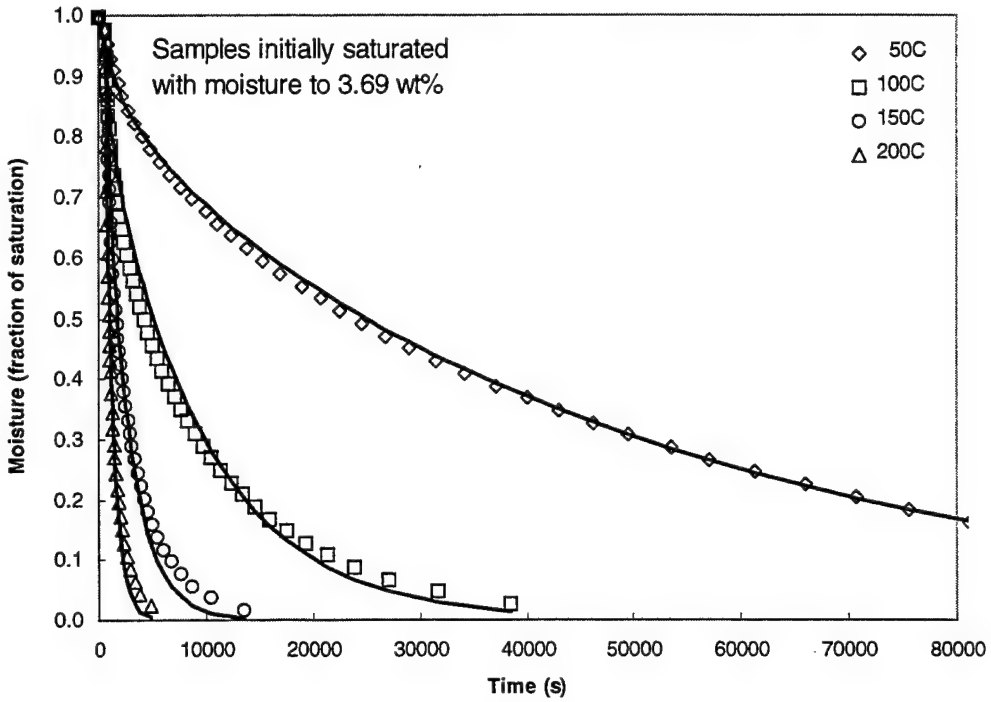

Figure 32. Measured (markers) and Predicted (curves) Moisture Content in 0.12-inch Thick Samples Undergoing Isothermal Drying at Different Temperatures.

SECTION 4

EVALUATION OF THE EFFECTIVENESS OF SILICON NITRIDE AS A MOISTURE BARRIER

NASA-Lewis Research Center (NASA-LeRC) has evaluated the effectiveness of silicon-nitride coatings to protect polyimide composites from both abrasion and oxidation [22]. Silicon nitride is also a proven moisture barrier as demonstrated by the electronics industry [23]. A program was conducted to determine if such a coating would be an effective moisture barrier for polyimide composites. Samples consisting of AFR700B resin, AFR700B/S2 glass, and AFR700B/carbon were coated with silicon nitride by NASA-LeRC; in addition uncoated samples were retained as controls. The samples were vacuum dried at 110°C to a constant weight and were then placed in a humidity cabinet at 85 percent RH/29.5°C. Unfortunately the daily weight gain of the coated samples was no different from that of the uncoated samples. Optical microscopy of the coating revealed the presence of numerous cracks and spalling locations.

SECTION 5
CONCLUSIONS AND RECOMMENDATIONS

5.1 CONCLUSIONS

- Thermomechanical and relaxation spectra data suggest that physical aging occurred in all aged specimens in a similar manner, regardless of aging environment.

- Increases in glass transition temperature and apparent rubbery storage modulus suggested additional crosslinking occurred as a result of aging in as-cured specimens.

- The decline in the glass transition temperature and changes in the relaxation spectra suggest molecular breakdown under prolonged hygrothermal exposure.

- Weight loss of specimens suggests that the presence of moisture can enhance thermal oxidative degradation.

- A decline in glass transition temperature can occur after exposure to saturated steam at temperatures as low as 100°C.

- Exposure of specimens to saturated steam at 200°C resulted in severe degradation.

- Imide linkages formed during cure may be highly strained and thus vulnerable to hydrolysis.

- The ultimate strength at 250°C was reduced by 38 percent after aging in saturated steam for 48 hours at 150°C.

- The ultimate strength at 300°C was reduced by 49 percent after aging in saturated steam for 48 hours at 150°C.

- Moisture diffusivity was modeled using absorption and desorption.

- Data suggests that a Fickian diffusion model is valid up to the point of sample blistering.

- Silicon nitride coatings contained cracks and spalling sites and did not protect the resin from moisture absorption.

5.2 RECOMMENDATION

- Additional work is required in the area of hydrolytic degradation of polyimides to understand the effect of degradation on mechanical performance.

SECTION 6

PUBLICATIONS/PRESENTATIONS

Rice, B. P. (1996). Recent Studies Concerning Hydrolytic Degradation of High-Temperature Polyimides. *Proceedings of High Temple Workshop XVI* (pp. U1-U23).

Rice, B. P. (1996). Hygrothermal Studies on Fluorinated Polyimides - A Physical Characterization. *Proceedings of 28th International SAMPE Technical Conference.*

Thorp, K. E. G., & A. S. Crasto. (1995). Hygrothermal Stability of Polyimide Resins and Composites. *Proceedings of American Society for Composites Tenth Technical Conference* (pp. 601-612).

Thorp, K. E.G., & A. S. Crasto. (1996). Hygrothermal Cycling of AFR700B. *Proceedings of High Temple Workshop XVI* (pp. V1-V30).

Thorp, K. E. G., A. K. Roy, & A. S. Crasto. (1996). The Effect of Isothermal Aging on the Relaxation Spectra of AFR700B. *Proceedings of 28th International SAMPE Technical Conference* (pp. 797-806).

Thorp, K. E. G., & A. S. Crasto. (1997). The Effect of Aging Environment on the Structure and Properties of AFR700B. *Proceedings of High Temple Workshop XVII* (pp. K1-K31).

SECTION 7

REFERENCES

1. Serafini, T. T., P. Delvigs, & G. R. Lightsey. (1972). Thermally Stable Polyimides from Solutions of Monomeric Reactants. *J. of Applied Polymer Science 16*(4) (pp. 905-915).

2. Garcia, Dana, & T. T. Serafini. (1987). FTIR Studies of PMR-15 Polyimides. *J. of Polymer Science: Part B: Polymer Physics 25* (pp. 2275-2282).

3. Johnston, James C., Mary Ann B. Meador, & William B. Laston. (1987). A Mechanistic Study of Polyimide Formation from Diester-Diacids. *J. of Polymer Science: Part A: Polymer Chemistry 25* (pp. 2175-2183).

4. Hay, J. N., J. D. Boyle, S. F. Parker, & D. Wilson. (1989). Polymerization of N-phenylnadimide: A Model for the Crosslinking of PMR-15 Polyimide. *Polymer 30* (pp. 1032-1040).

5. Scola, D., & J. Vontell. (1988). High-Temperature Polyimides, Chemistry and Properties. *Polymer Composites 9*(6) (pp. 443-452).

6. Curliss, D. B. (1996). Environmental Effects on High Performance Polymers and Composites. *Proceedings of the High Temple Workshop XVI* (pp. H1-H16).

7. Cornelia, D. (1994). Hygrothermal Performance of Polyimides. *Proceedings of 39th International SAMPE Symposium* (pp. 917-929).

8. Thorp, K. E. G., & A. S. Crasto. (1995). Hygrothermal Stability of Polyimide Resins and Composites. *Proceedings of the American Society for Composites 10th Technical Conference* (pp. 601-612).

9. Murphy, P., et al. (1994). Nitrogen-15 Solid State NMR Studies of the Cure and Degradation of Polyimide Films under Temperature and Humidity Stresses. *Macromolecules 27* (pp. 279-286).

10. Struik, L. C. E. (1978). *Physical Aging in Amorphous Polymers and Other Materials.* Elsevier Scientific Publishing Co., Amsterdam.

11. Venditti, R. A., & J. K. Gillham. (1992). Physical Aging Deep in the Glassy State of a Fully-Cured Polyimide. *Journal of Applied Polymer Science 45* (pp. 1501-1516).

12. Pryde, C. A. (1989). Polyimide Hydrolysis; Measurement by Fourier Transform-IR Spectroscopy. *Polymeric Materials for Electronics Packaging and Interconnection* (pp. 57-66).

13. Odian, G. (1970). *Principles of Polymerization*. McGraw Hill Book Company.

14. Ferry, J. D. (1980). *Viscoelastic Properties of Polymers*, Third Edition. John Wiley & Sons, Inc. (pp. 83-84).

15. Iarve, E. V. (1996). Spline Variational Three Dimensional Stress Analysis of Laminated Composite Plates with Open Holes. *Intl. J. Solids Structures 33*(14) (pp. 2095-2118).

16. Johnson, L. W., & R. D. Riess. (1982). *Numerical Analysis*, 2nd Ed. Addison-Wesley Publishing Co. (Section 2.5, p. 71).

17. Press, W. H., et al. (1989). *Numerical Recipes*. Cambridge University Press, New York (Section 2.3, p. 31).

18. Sperling, L. H. (1992). *Introduction to Physical Polymer Science*, Second Edition. John Wiley & Sons, Inc. (pp. 398-402).

19. Harrell, E. R., Jr., & R. P. Chartoff. (1977). Effects of Thermal and Mechanical History on the Viscoelastic Properties of Rigid Poly(vinyl Chloride). *J. Macromol. Sci. - Phys. B14*(2) (277-305).

20. Bauwens-Crowet, C., & J-C. Bauwens. (1979). The Relationship between the Effect of Thermal Pre-Treatment and the Viscoelastic Behaviour of Polycarbonate in the Glassy State. *Journal of Materials Science 14* (1817-1826).

21. Price, W. A., B. P. Rice, A. S. Crasto, & K. A. Thorp. (1995). Hygrothermal Aging of Imide Composites. *Proceedings of the High Temple Workshop XV* (pp. S1-S24).

22. Harding, D., J. Sutter, M. Schuerman, & E. Crane. (1994). Oxidation Protective Barrier Coatings for High-Temperature Polymer Matrix Composites. *J. Mater. Res. 9*(6) (p. 1584).

23. Kern, W., & R. S. Rosler. (1977). *J. Vac. Sci. Technol. 14* (p. 1082).